Lecture 2 041019

- Slides will be available at:

https://www.fisgeo.unipg.it/~fiandrin/didattica_fisica/cosmic_rays1920

Zeeman splitting

- A probe which is widely used for measurements of the parallel component of the field, in our galaxy, in starbursts galaxies and few nearby galaxies B_p.
- It's a way to determine field strength in gas clouds from the emission line of 21 cm, or from maser emission from dense core like galactic nuclei.

- The interacting energy U between the external magnetic field and the magnetic dipole 'nuclei-electron' is:

$$\left.\begin{aligned} U &= -m \cdot B \\ m &= -\mu_B \cdot \frac{L}{\mathrm{h}} \\ L &= m_l \cdot \mathrm{h} \end{aligned}\right\} \longrightarrow U = m_l \cdot \mu_B \cdot B$$

Which is the energy difference between the two splitted lines.

Zeeman splitting

- Let f_0 be the frequency of the unshifted spectral line, then the frequencies of the splitted lines will be:

$$f = f_0 \pm \frac{e \cdot B}{4\pi \cdot m_e \cdot c}$$ (5), hence measuring the frequencies of the spectral lines, the parallel component of the field is defined.

- **From the change of the circular polarization we extract the average field direction**.

Polarized emission at optical, infrared and radio synchrotron emission

Starlight polarization:

- Optical linear polarization is the result of scattering from elongated dust grains in the line-of-sight, which are collimated in the interstellar magnetic field (Davies-Greenstein effect).
- Dust grains are not spherical, their long axis is perpendicular to the field and they are spinning rapidly with rotation axis along the magnetic field.

- E vector runs parallel to the field because grains tend to absorb light polarized at the direction of the long axis, thus we measure the vertical component $B_{\perp}$.
- Measurements from thousand of stars
- **Reliable detector for distances <3kpc and mainly for small-scale fields.**

Polarized emission at optical, infrared and radio synchrotron emission

Infrared polarized emission of clouds and dust:

- The same grains that polarize starlight also radiate in the infrared. This thermal emission is polarized owing to the shape of grains as presented above.

- Similarly we estimate the vertical component of the magnetic field $B_{\perp}$.

Synchrotron emission:

- Accelerating electrons gyrating magnetic field lines radiate radio synchrotron emission.

Polarized emission at optical, infrared and radio synchrotron emission

- Significant tracer of magnetic field's strength and orientation, of external galaxies (Beck 2009) and our Milky Way, by measuring the total radio intensity and polarization respectively.
- Polarized emission traces ordered fields while unpolarized synchrotron emission indicate turbulent fields with random directions.
- We estimate the vertical component of the field $B_{\perp}$.
- The estimation is based on the distribution of relativistic electrons in a range of energies: * widely assumed power law distribution of electrons combined with the equipartition of energy density between magnetic field and cosmic rays lead to:

$$j_{syn} \propto B^{2/7}_{\perp}$$

Polarized emission at optical, infrared and radio synchrotron emission

Dataset	measures what?	ancillary data	data points	region covered
Synchrotron emission	$B_\perp$ orientation	n_{cre}	3×50k (WMAP)	full sky
RM: pulsars	$B_\parallel$	n_e	529	mainly disk; $\lesssim 10$ kpc
RM: X-Galactic	$B_\parallel$	n_e	∼1500	roughly uniform
Starlight polarization	$B_\perp$ orientation	grain physics	∼10k	mainly disk; $\lesssim 3$ kpc
Zeeman splitting	$B_\parallel$ *in situ*	none	∼100s	near quadrant

Table 1: Detectors of galactic magnetic fields.

Best probes for a large-scale field in our galaxy:
RM and Zeeman splitting.
The other probes good at revealing field details.

Magnetic field structure of Milky Way

Galactic disk:

- Ordered (regular or anisotropic) and turbulent field components.
- Large-scale pattern in disk has a strong azimuthal component.
- Small-scale structures also appear.
- Approximately the field follows the logarithmic spiral arms having a pitch angle 10^{o} . Parallel to the adjacent gas.
- Always clockwise in the arm region. Anti-clockwise in the interarm regions displaying field reservals.
- Stronger field and polarized emission in interarm regions .
- Strength near the sun : $6\mu G$ (Beck 2009).
- Norma arm : $4\mu G$.

Magnetic field structure of Milky Way

- Magnetic field in arms is passive to dynamics.

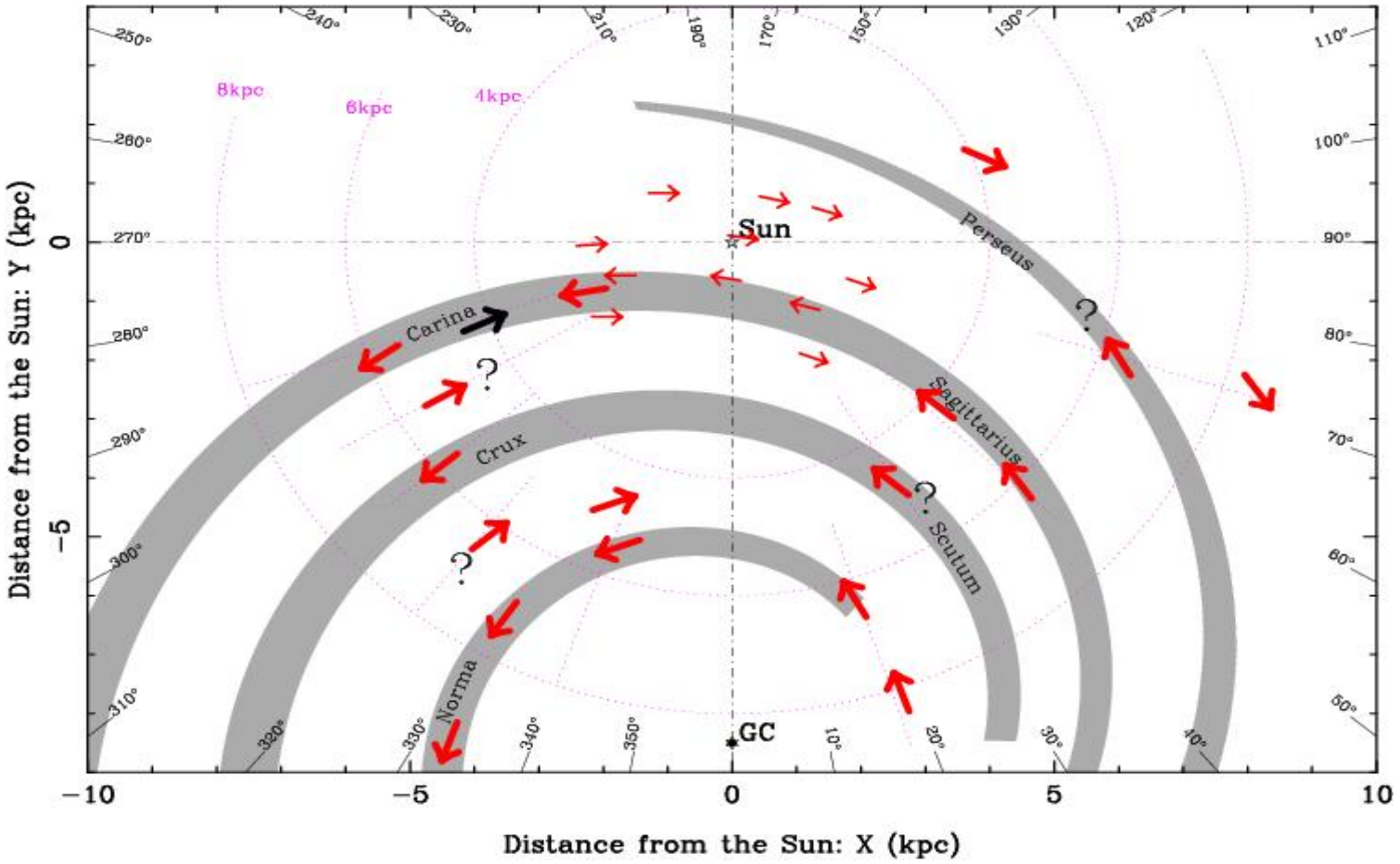

Figure 5: Field orientation in arm and interarm regions in Galaxy.

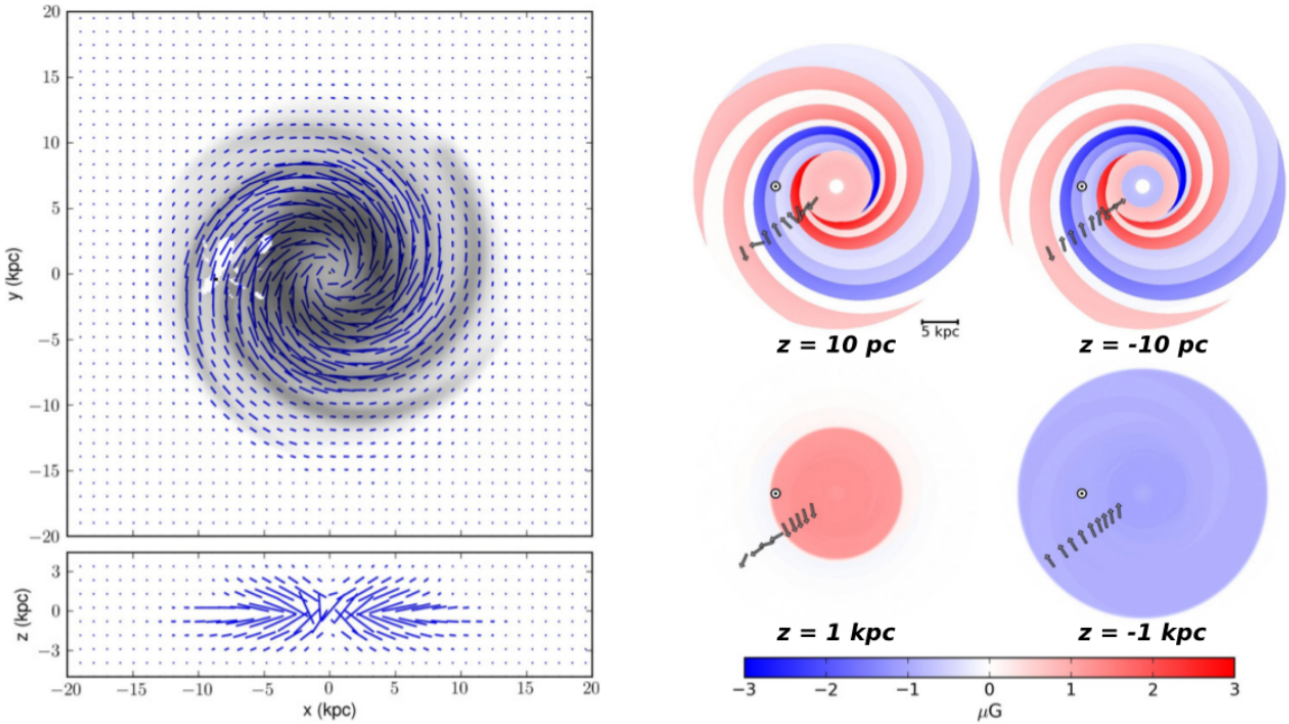

Figura 2.8: Le figure, tratte dall'articolo di Jansson & Farrar [30], mostrano la struttura del campo magnetico della nostra Galassia, ricavate secondo il modello elaborato dagli stessi autori. L'immagine a sinistra descrive la distribuzione delle direzioni e dell'intensità del campo magnetico come sarebbero viste da un osservatore esterno alla galassia. Mentre, l'immagine a destra è una raffigurazione schematica della struttura del campo magnetico galattico a diverse altezze dal piano galattico. D. Di Bari, Tesi di laurea, 2015

- Intensità media nel piano galattico: 3-6 μGauss
- Coerenti su scale di 1-10 pc

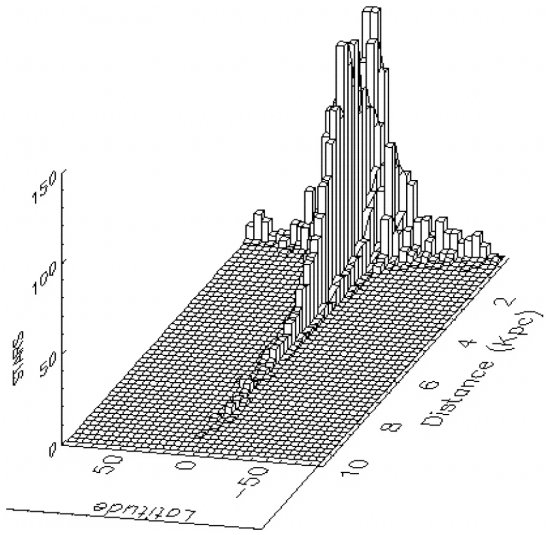

Polarizzazione della luce delle stelle: *local field // arm*

- 9000 stars have polarization measured
- mostly nearby (1~2kpc)
- polarization percentage increases with distance

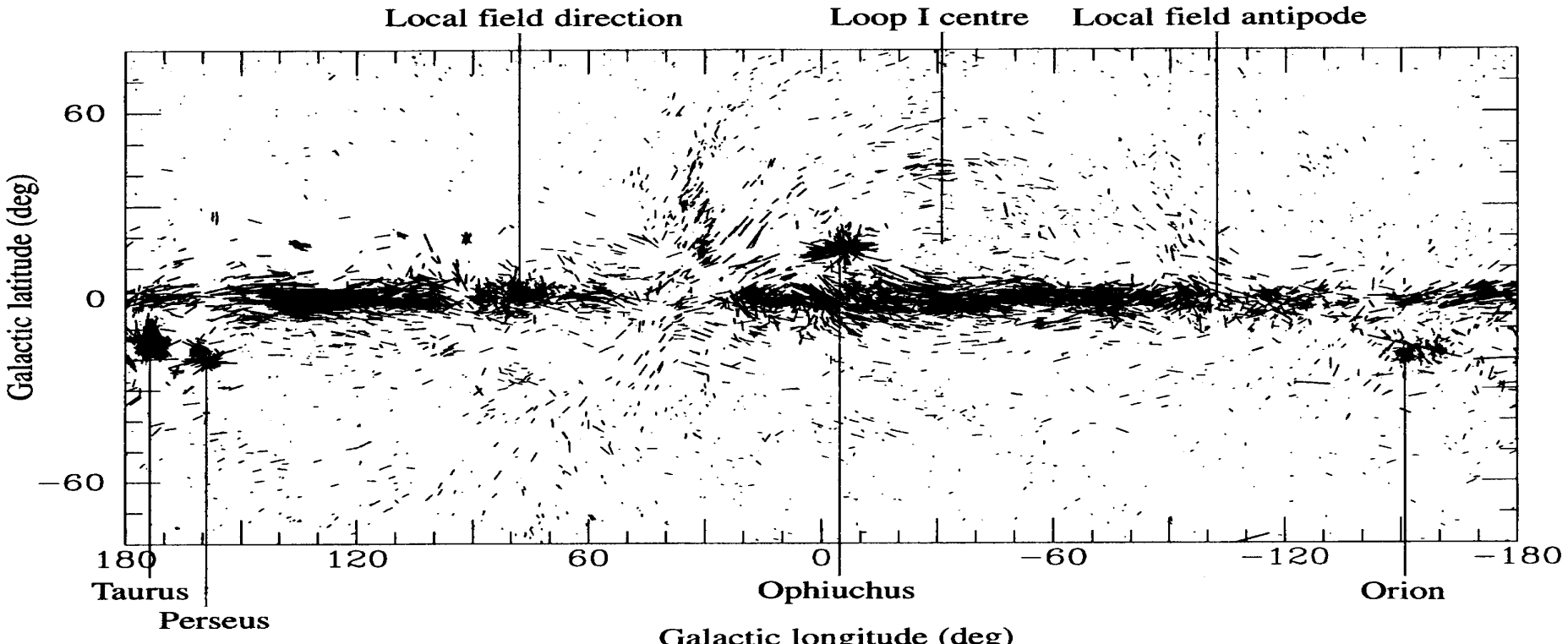

Zweibel & Heiles 1997, Nature 385,131 Berdyugin & Teerikorpi 2001, A&A 368,635

- Each line represents the polarization measurement for a star; length is proportional to the fractional polarization and orientation is in the max polariz., which is || B.
- Within 10^o from galactic plane, B is generally || to the galaxy plane
- Can be used to derive $B_o/\delta B$ from uniformity of the optical pol data: $B_o/\delta B \sim 0.3 - 1$.
- At positions at 10^o off the gal plane there is a considerable small-scale structure
- At high gal latitudes several local interstellar bubbles each produced by multiple supernovae (eg Loop I)

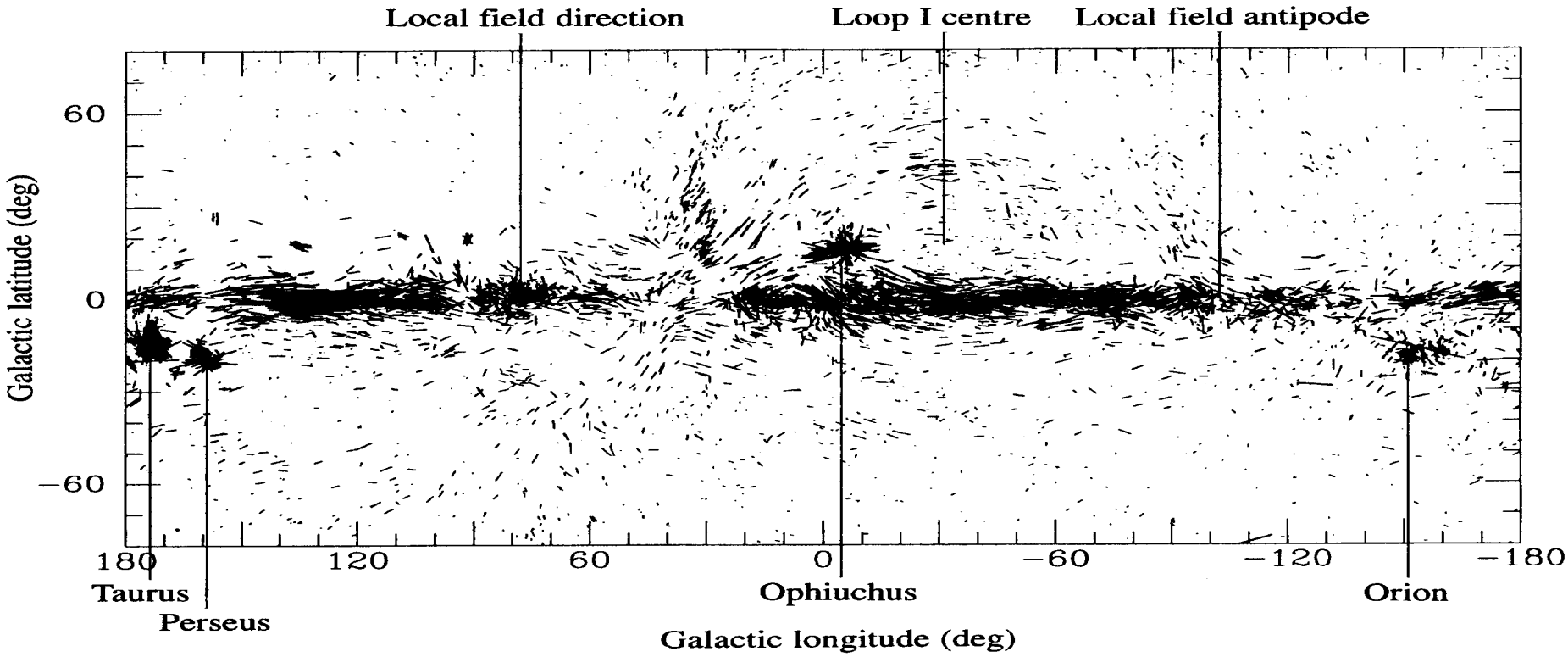

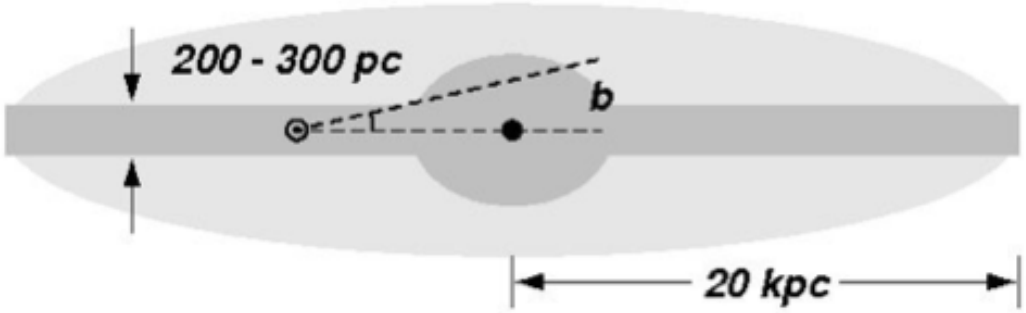

What is the magnetic field as a function of the distance from the galactic center? Also above and below the galactic plane.

The average magnetic field decreases when we move away from the Galactic center. Measurements are fit with different functions. The easiest one is just linear, based on the the local 2 μG field. In such a Case the field at 4 kpc from the galactic center would be
2 μG 8.5/4 = 4.25 μG.

It is more difficult to estimate the field in the galactic magnetic halo. Cosmic rays, although accelerated in the plane, diffuse away from it and carry with them magnetic field as they do in the Solar system. Most models prefer an exponential dependence with an exponent between 0.5 and 1 kpc. Since the field is stronger around the galactic center and decreases with distance from it the halo would form an ellipse. The details are being investigated now.

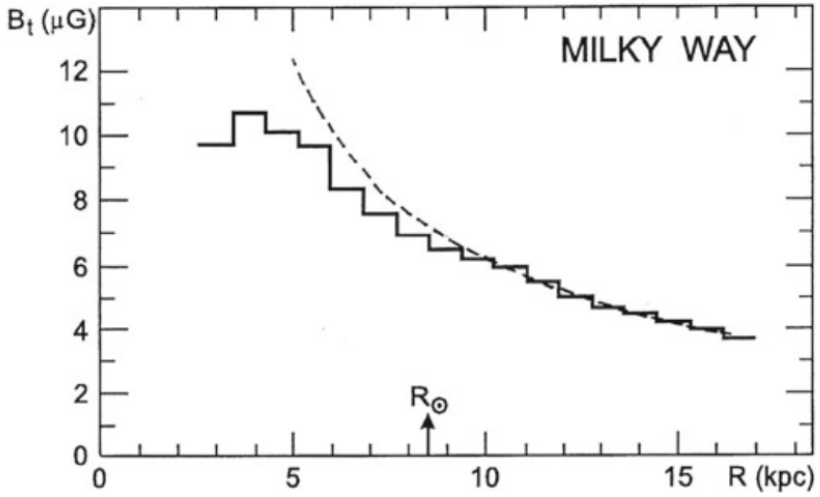

Fig. 2.9 Total magnetic field strength in the Galaxy as a function of the distance from the galactic center. The position of the Sun is indicated by the *arrow* (Battaner et al. 2007). Courtesy of Prof. E. Battaner

Fig. 2.10 The direction and strength of the regular magnetic field in the Galactic plane is represented by the length and direction of the arrows. The intensity of the field inside the circle of radius 4 kpc representing the bulge is assumed to be 6.4 μG (Prouza and Smída 2003). Courtesy Dr. M. Prouza and Dr. R. Smída

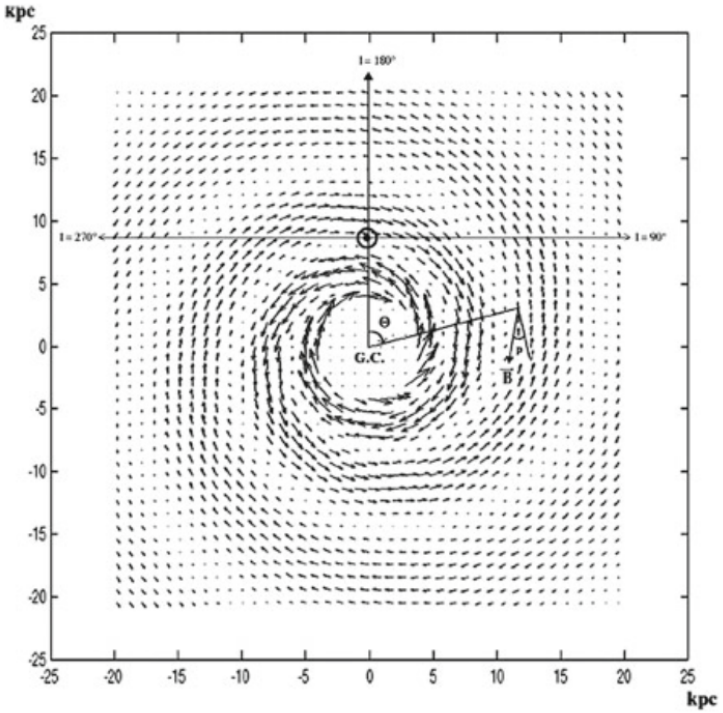

Galactic Magnetic Field

- Galactic magnetic field is irregular in the sense that it shows different intensities and directions distributed randomly in the galaxy
- Usually, B is decomposed in two components:
  - Regular, large scale average field B_o
  - Random small scale irregularities $\delta B(x)$ of the field

$$B(x) = Bo + \delta B(x)$$

Description of the magnetic fields

When B field has irregularities and gradients which are randomly distributed, it can represented as

$$\mathbf{B}(\mathbf{r},t) = \mathbf{B}_0 + \delta\mathbf{B}(\mathbf{r},t)$$

With $\mathbf{B}_0$ average, large scale field and $\delta\mathbf{B}$ random field irregularities.
Since $\delta\mathbf{B}$ is random, then $\langle\delta\mathbf{B}\rangle = 0$, while $\langle\delta B^2\rangle \neq 0$

The average field energy density is $\langle u\rangle = \langle B^2\rangle/8\pi$ in Gauss units

$$\langle B^2\rangle = B_0^2 + \langle\delta B^2\rangle + \underbrace{2\mathbf{B}_0\bullet\langle\delta\mathbf{B}\rangle}_{=0}$$

Consider a fluctuating field B(t). If B(t) is random, it is drawn from a probability distribution P(B). The instantaneous value cannot be predicted, but averages can be precisely defined.
The expectation value of a function of B, f(B), can be defined as an integral over time, or over the distribution

$$\langle f(B) \rangle = (1/T) \int_{-T/2}^{T/2} f(B(t))\, dt$$

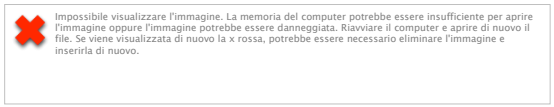

The average is $\langle B \rangle = \int B \cdot P(B) dB$ and the variance $\sigma^2 = \langle B^2 \rangle - \langle B \rangle^2$

Time dependence

The probability distribution contains no information about the time variation $V(t)$

This can be described by the *autocovariance function* $\Psi_V(\tau)$

$$\Psi_V(\tau) = \langle V(t)\ V(t-\tau) \rangle = \lim_{T \to \infty} (1/T) \int_{-T/2}^{T/2} V(t) V(t-\tau) dt$$

When the autocovariance is normailized by the variance σ, then it is called the *autocorrelation function*.

It ranges from 1 to -1.

The rate at which the autocorrelation function decays as a function of τ, indicates how fast $V(t)$ varies with time.

The Fourier transform of the fluctuating quantity $V(t)$ is

$$\hat{V}(f) = \lim_{T\to\infty} \int_{-T/2}^{T/2} \exp(2\pi i f t) V(t) dt \qquad (1)$$

The inverse transform is

$$V(t) = \lim_{F\to\infty} \int_{-F/2}^{F/2} \exp(-2\pi i f t) \hat{V}(f) df \qquad (2)$$

The Fourier transform is also a random variable.

The *power spectral density* $S(f)$ is defined in terms of the Fourier transform $\hat{V}(f)$

$$S(f) = \langle |\hat{V}(f)|^2 \rangle = \langle \hat{V}(f)\, \hat{V}^*(f) \rangle$$

$\hat{V}^*(f)$ is the complex conjugate $i \to -i$

$$S(f) = \lim_{T\to\infty} \int_{-T/2}^{T/2} \exp(2\pi i f t) V(t) dt \int_{-T/2}^{T/2} \exp(-2\pi i f t') V(t')\, \mathbf{dt'}$$

The Fourier transform is defined for positive and negative frequency. If it is defined only for positive frequency, the lower limit is 0, and a factor 2 is introduced in (2).

The power spectrum S(*f*) is related to the autocovariance function by the *Wiener-Khinchin theorem*: Its Fourier transform is equal to the autocovariance $\Psi_V(\tau)$.

$$\int_{-\infty}^{\infty} S(f)\exp(-2\pi i f\tau)\, df = \langle V(t)\, V(t-\tau)\rangle \qquad (3)$$

Conversely, the Fourier transform of the autocovariance gives the power spectrum.

As the autocorelation function decays more slowly, the the power spectrum decays faster and *vice versa*.

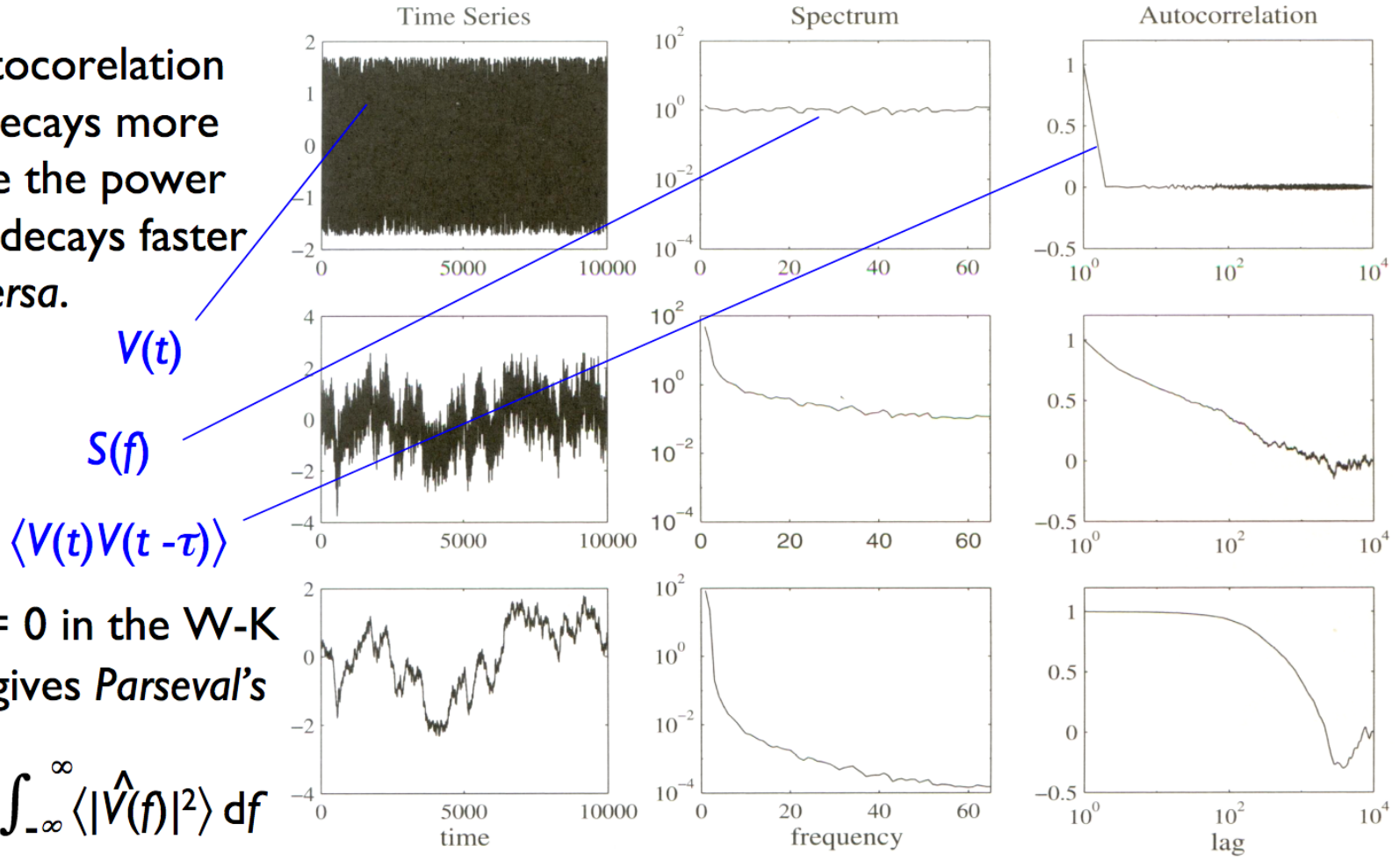

Taking $\tau = 0$ in the W-K theorem gives *Parseval's theorem*

$$\langle |V(t)|^2 \rangle = \int_{-\infty}^{\infty} \langle |\hat{V}(f)|^2 \rangle\, df$$

As an example of the use of the Wiener-Khinchin theorem, consider a relaxation process defined by a relaxation time τ_0.

The relaxation is defined by an exponentially-decaying autocorrelation function

$$\Psi_V(\tau) = \Psi_V(0) \exp\left[-|\tau|/\tau_0\right]$$

From the W-K theorem $\int_{-\infty}^{\infty} S(f)\exp(-2\pi i f\tau)\, df = \langle V(t)\, V(t-\tau)\rangle = \Psi_V(\tau)$

The inverse relation is $S(f) = \int_{-\infty}^{\infty} \Psi_V(\tau) \exp(2\pi i f\tau)\, d\tau$

$$= \int_{-\infty} \Psi_V(0) \exp\left[-|\tau|/\tau_0\right] \exp(2\pi i f\tau)\, d\tau$$

$$= \Psi_V(0)\{\tau_0/(1 + \tau_0^2 f^2)\}$$

The power spectral density corresponding to a single exponential decay is therefore a Lorentzian spectrum with a corner frequency of $1/\tau_0$, and a $1/f^2$ frequency dependence at higher frequency

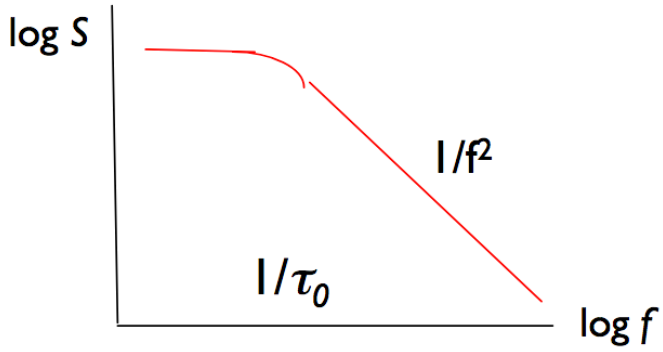

Power Spectrum

- Field is described as a superposition of plane waves
- Power spectrum is the Fourier transform of the random field
- It gives the energy of the Fourier component at a given wave number k and/or at a given frequency w.
- The wave number k gives the scale of length $\lambda = 2\pi/k$ over which the k-th component is $\neq 0$
- The highest is k, the smallest is the region where the perturbation $\delta B(k)$ acts

- Why is it important to CR propagation?
- Particles interact with field irregularities with a spatial scale λ of the same size as their Larmor through the so-called “cyclotron resonance”
- As a consequence, CR particles are scattered randomly and their motion can be described as a diffusion process which depends on power spectrum of the B field

Power Spectrum

- Most turbulence theories involve the processes by which energy injected into a medium at large spatial scales is converted into motions at smaller and smaller spatial scales (or eddies) until reaching scales at which the turbulence energy interacts directly with individual plasma particles and causes heating.
- Generally speaking, the PSD is described by power laws in k, that depends on k.

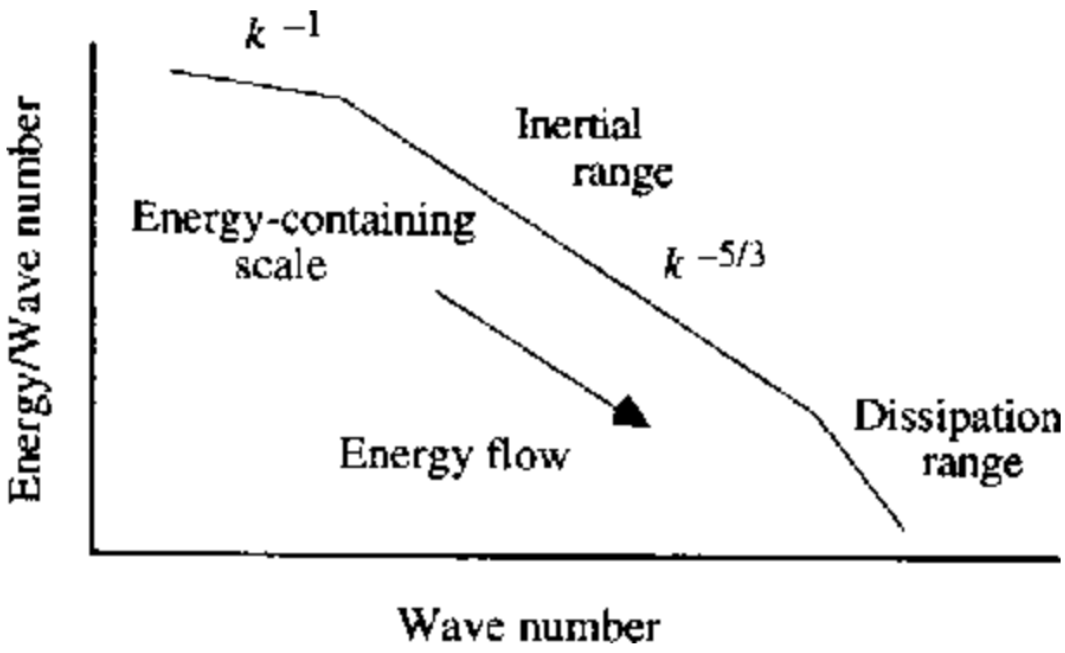

Magnetic field power spectrum of solar wind

Power Spectrum

- The process by which wave energy moves to smaller wavenumbers is sometimes called a “turbulent cascade”. This process can be mimicked to some degree by stirring a fluid and watching it come into equilibrium. The range of wavenumbers over which the turbulence energy cascades to smaller wavenumbers is called the inertial range. Using both gasdynamic (GD) and MHD theory, it can be shown using energy balance arguments that the power spectrum in the inertial range should be a power law with spectral index in the range 3/2 - 5/3.
- Kinetic theory is required to understand the dissipation of the turbulence in the so-called ``dissipation range'' at small spatial scales.

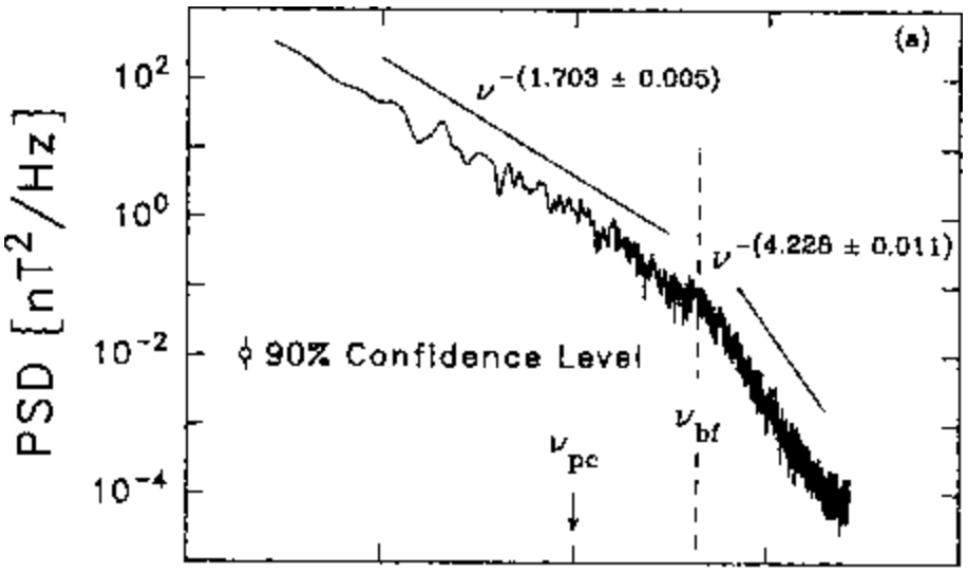

Typical spectrum of interplanetary magnetic power spectrun in a given period of the solar activity

Power Spectrum

- The power spectrum of the random component of the galactic magnetic field is essential to explain to diffusion of cosmic rays in the galaxy through collisionless scattering over the irregularities

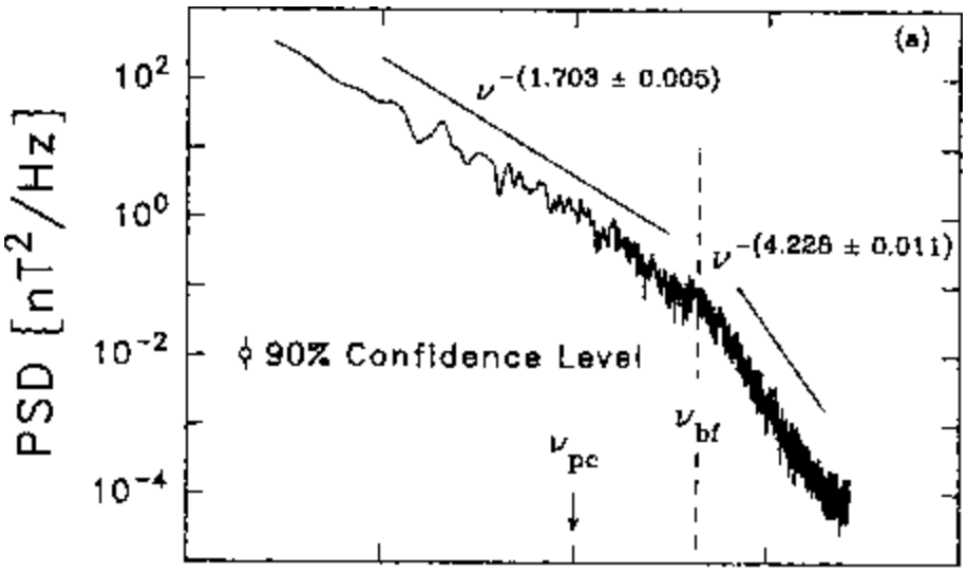

Typical spectrum of interplanetary magnetic power spectrun in a given period of the solar activity

Random field δB

- Measurements (eg starlight polariz.) shows that the random field exceeds the mean field by a large factor
- The random field lies mainly parallel to the mean field, while the perp component is much lower $\langle \delta B_p \rangle / \langle \delta B_n \rangle \sim 4$
- However from the measurements it's hard to determine the B field power spectrum density

SNR in the galaxy

- The galaxy contains ~10^{11} stars
- The more massive are relevant to the CR
- They explode as SN
- The Supernovae Remnant (SNR) shock wave in a magnetized medium accelerates CR, i.e. high energy CR source
- Spatial distribution and rate of explosion are important

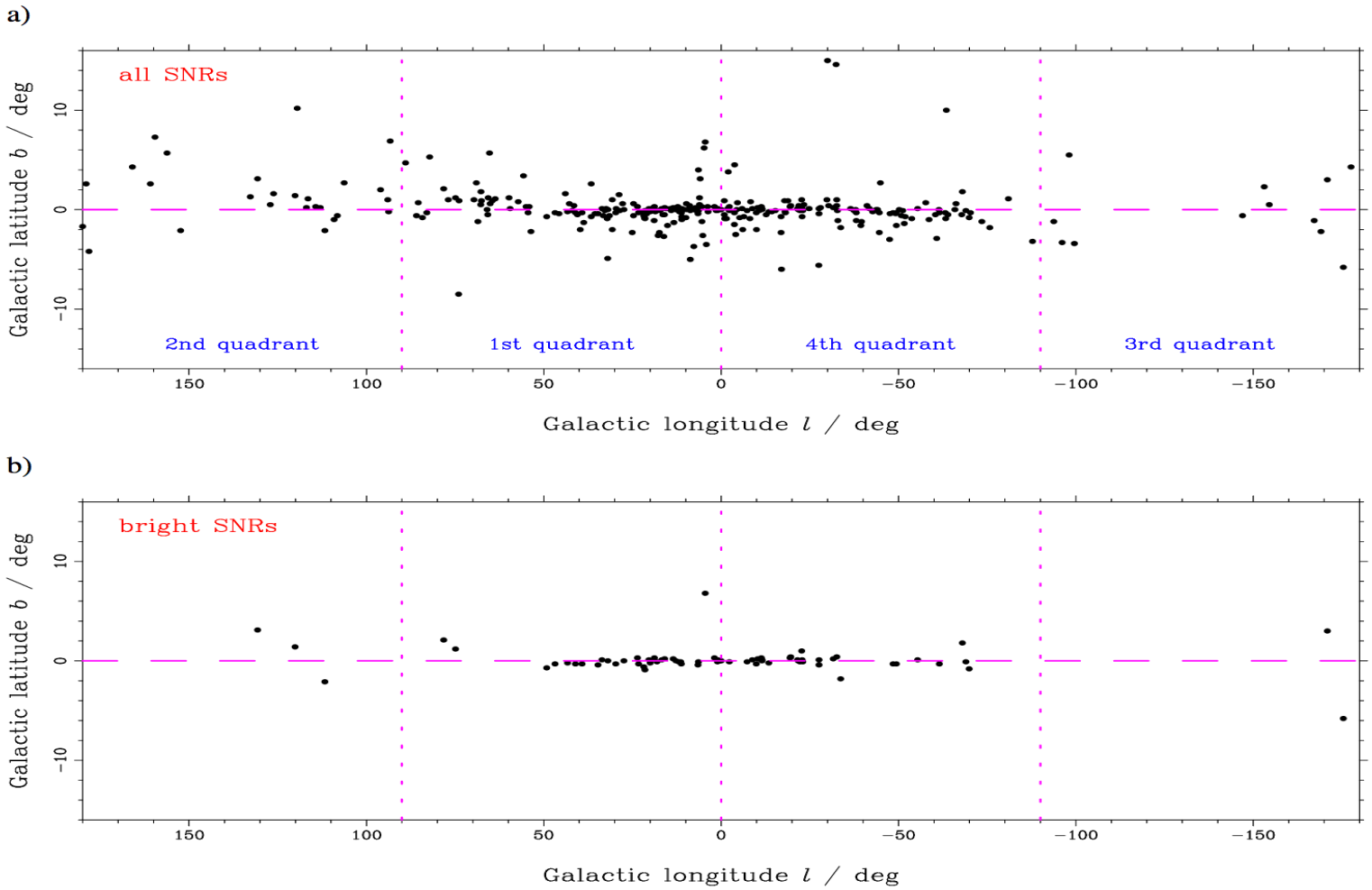

Figure 4. The distribution of SNRs in Galactic coordinates of all 294 catalogued SNRs for: (a) all SNRs, (b) the 69 'bright' SNRs with a surface brightness above 10^{-20} W m^{-2} Hz^{-1} sr^{-1}. Note that the latitude scale is exaggerated.

294 known SNR (2014)

Mostly in the galactic disk and around the bulge

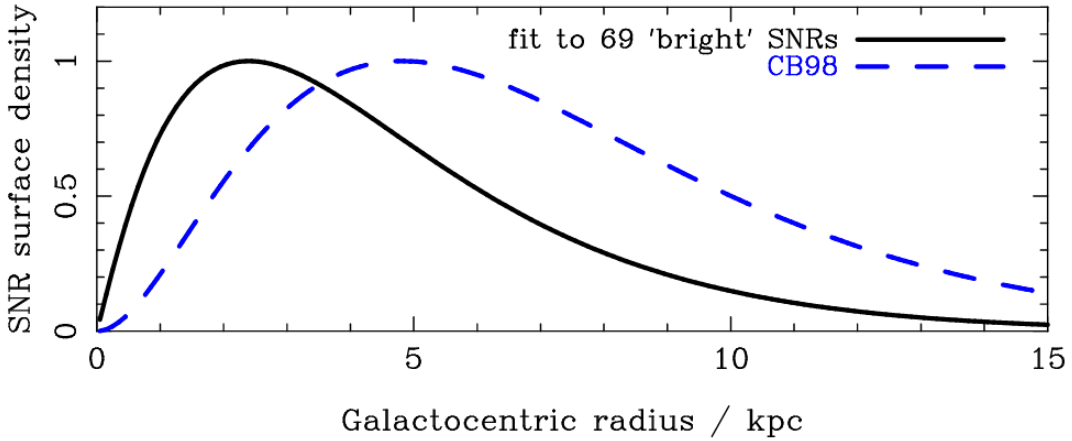

Figure 9. Normalised surface density of SNRs with Galactocentric radius for power-low/exponential models: (i) solid line, the best fit to *l*-distribution of 69 bright SNRs, and (ii) dashed line, from CB98.

Radial distribution of the surface density of SNR

- ✓ No SN have exploded in our galaxy since the beginning of modern observations
- ✓ We observed just one SN explosion in the Large Magellanic Cloud in 1987 (SN1987A)
- ✓ The extimated average is ~3/century

The Galactic Center

Our view (in visible light) towards the galactic center (GC) is heavily obscured by gas and dust

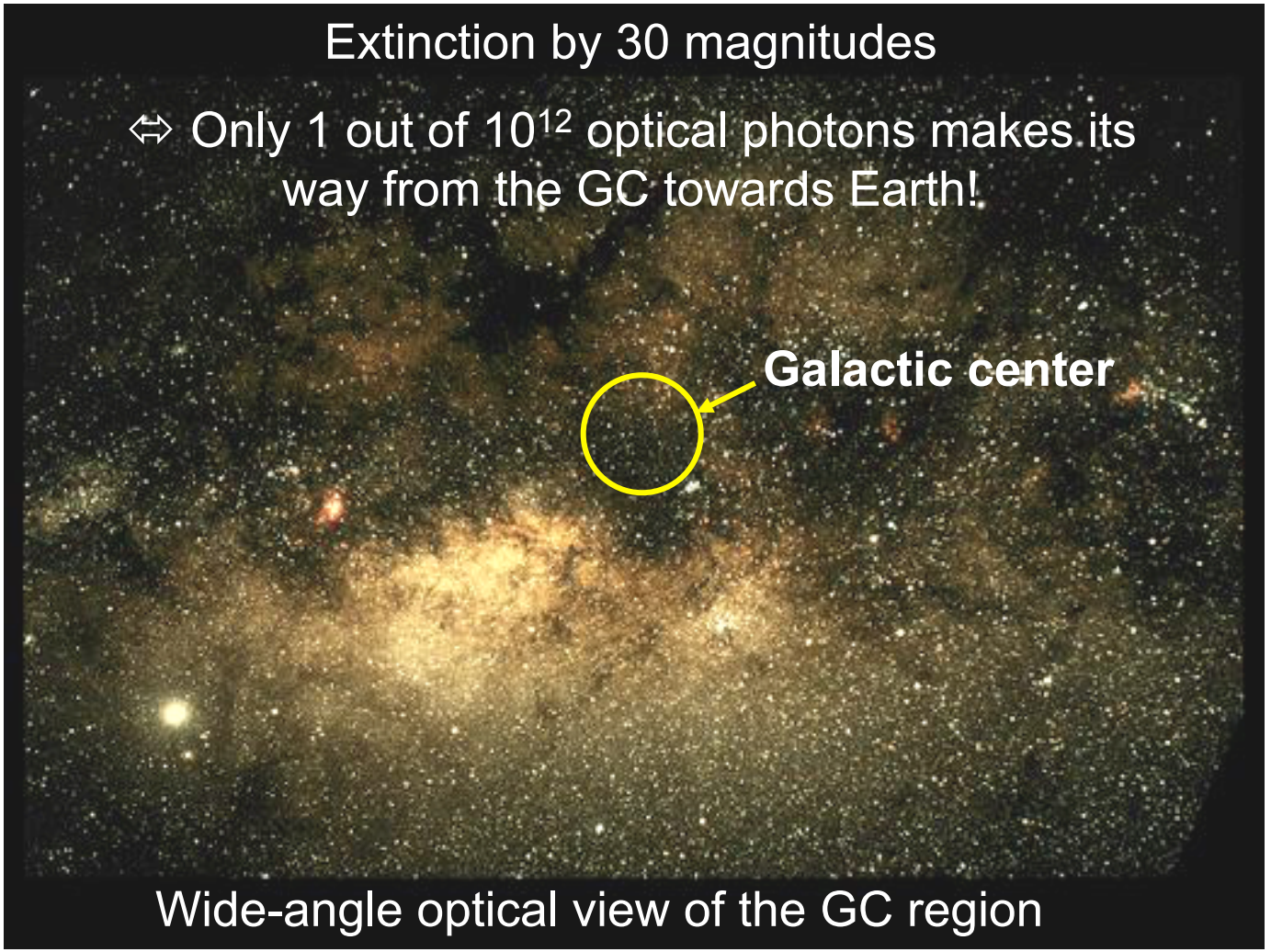

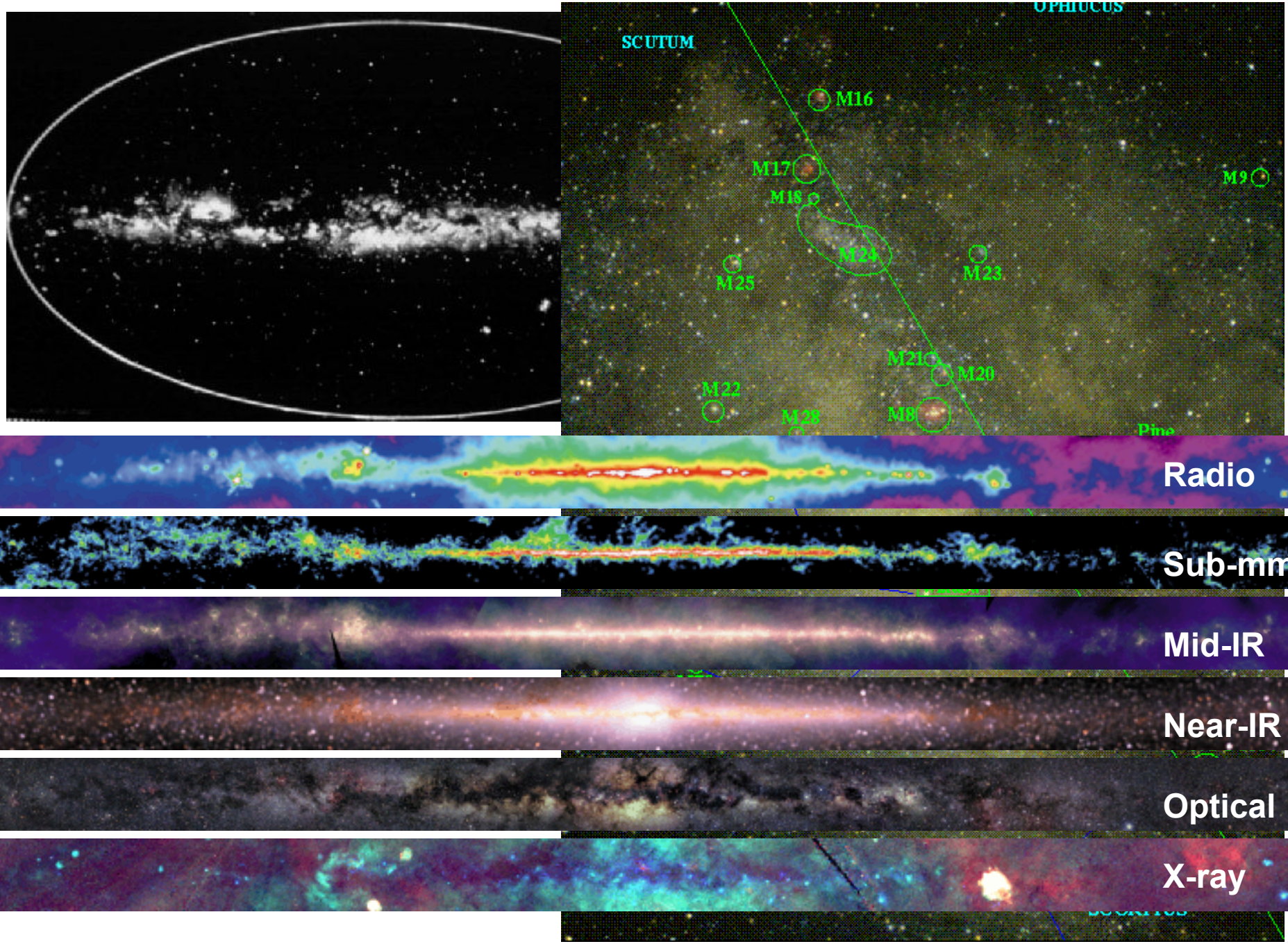
SCUTUM
M16
M17
M18
M24
M25
M23
M9
M21
M20
M22
M28
M8
Radio
Sub-mm
Mid-IR
Near-IR
Optical
X-ray

Need to observe the GC in the radio, infrared, or X-ray range

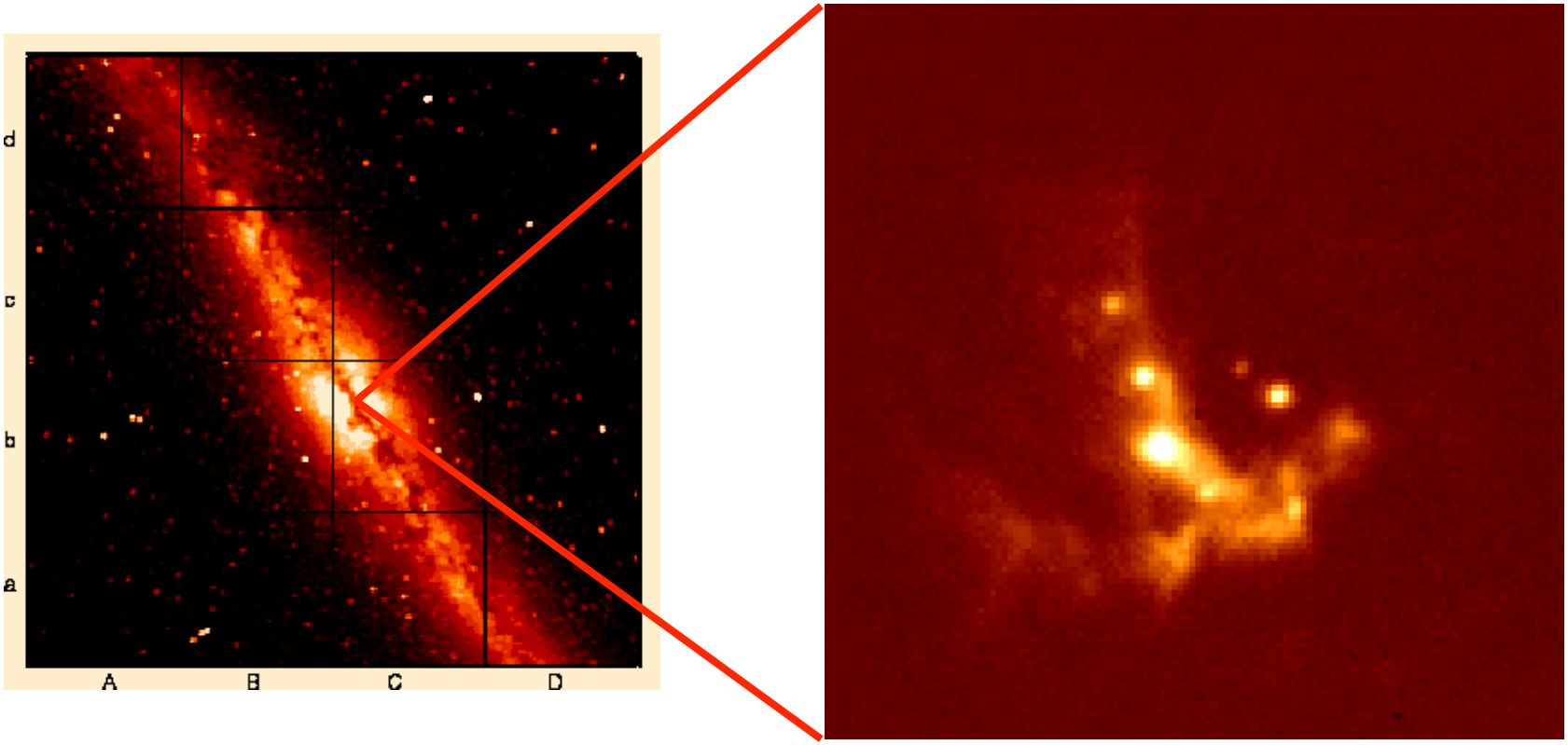

Infrared images

Central 2 pc

Image from the Very Large Array (VLA) radio telescope in New Mexico.

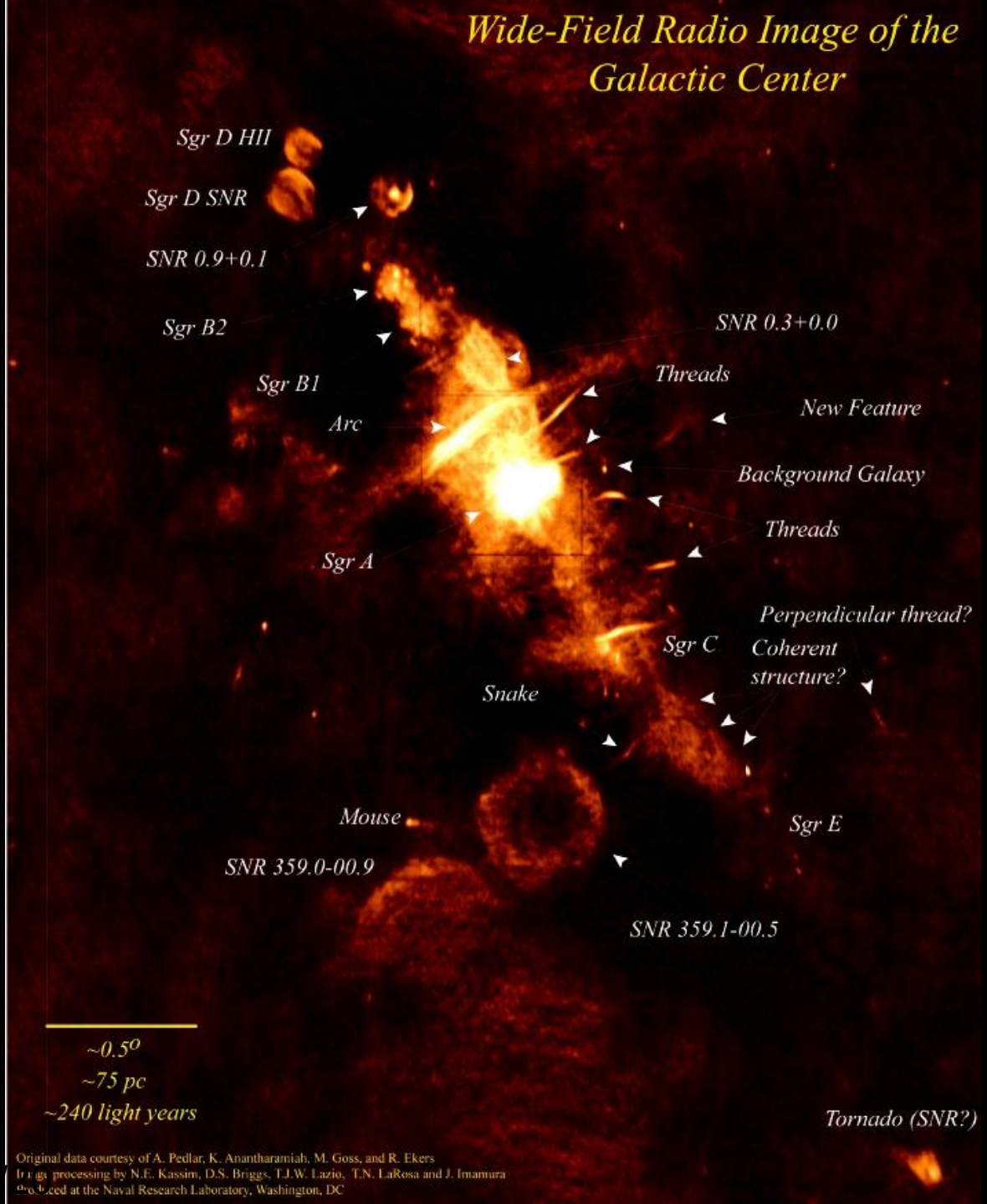

Radio View of the Galactic Center

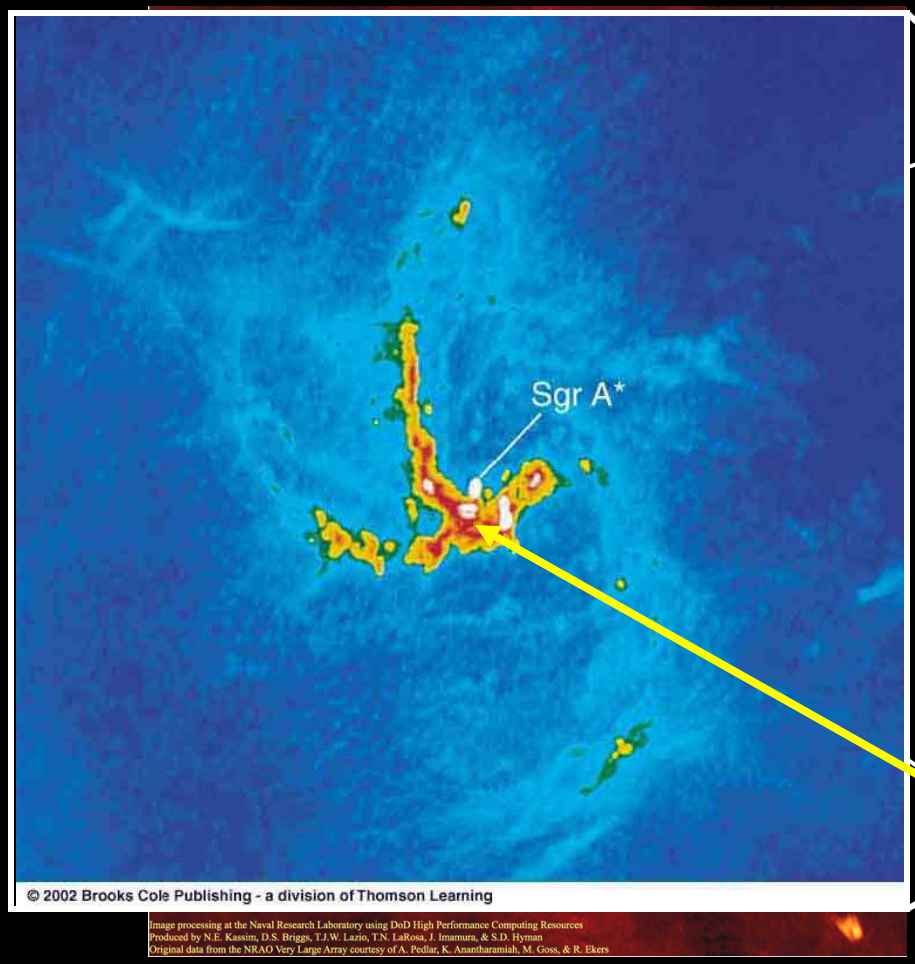

Many supernova remnants; shells and filaments

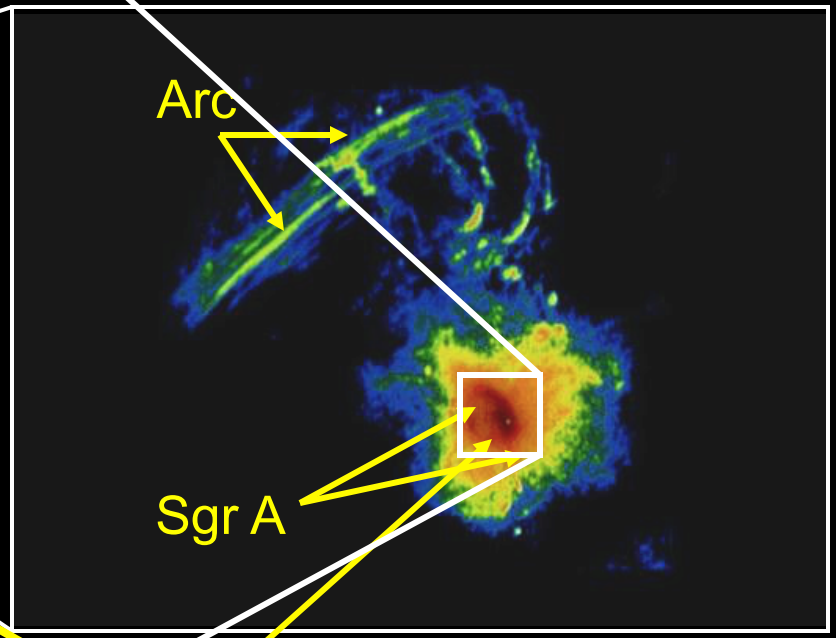

Sgr A*: The Center of our Galaxy

Fast rotation of spiral filaments around Sgr A*

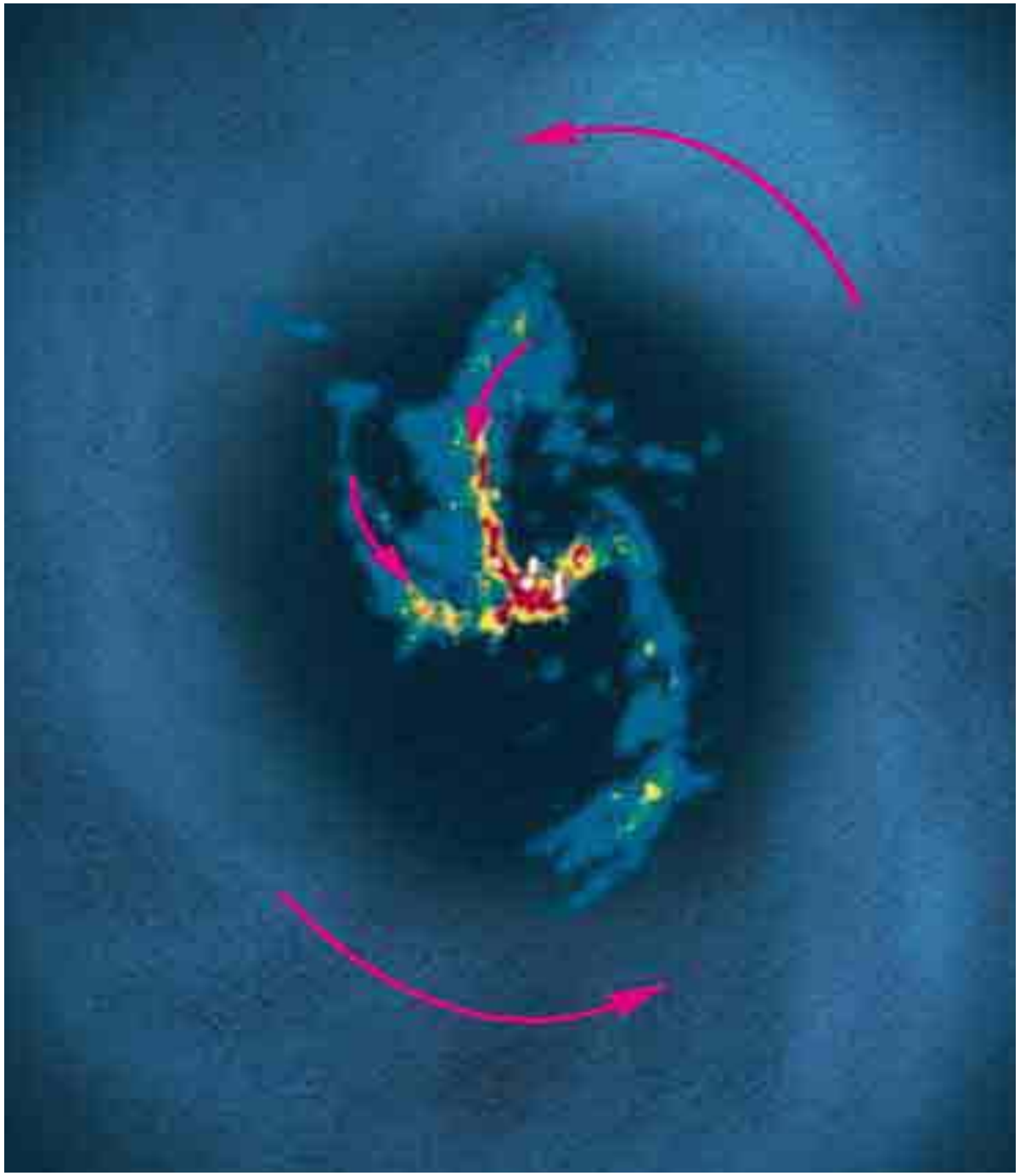

The Galactic Center at 2.2 microns

If one looks at this region with big telescopes and near-infrared cameras one can see lots of stars. If one takes pictures every year it seems that some stars are moving very fast (up to 5000 km/s – 2% of light speed!-). The fastest stars are in the very center - the position marked by the radio nucleus Sagittarius A* (cross).

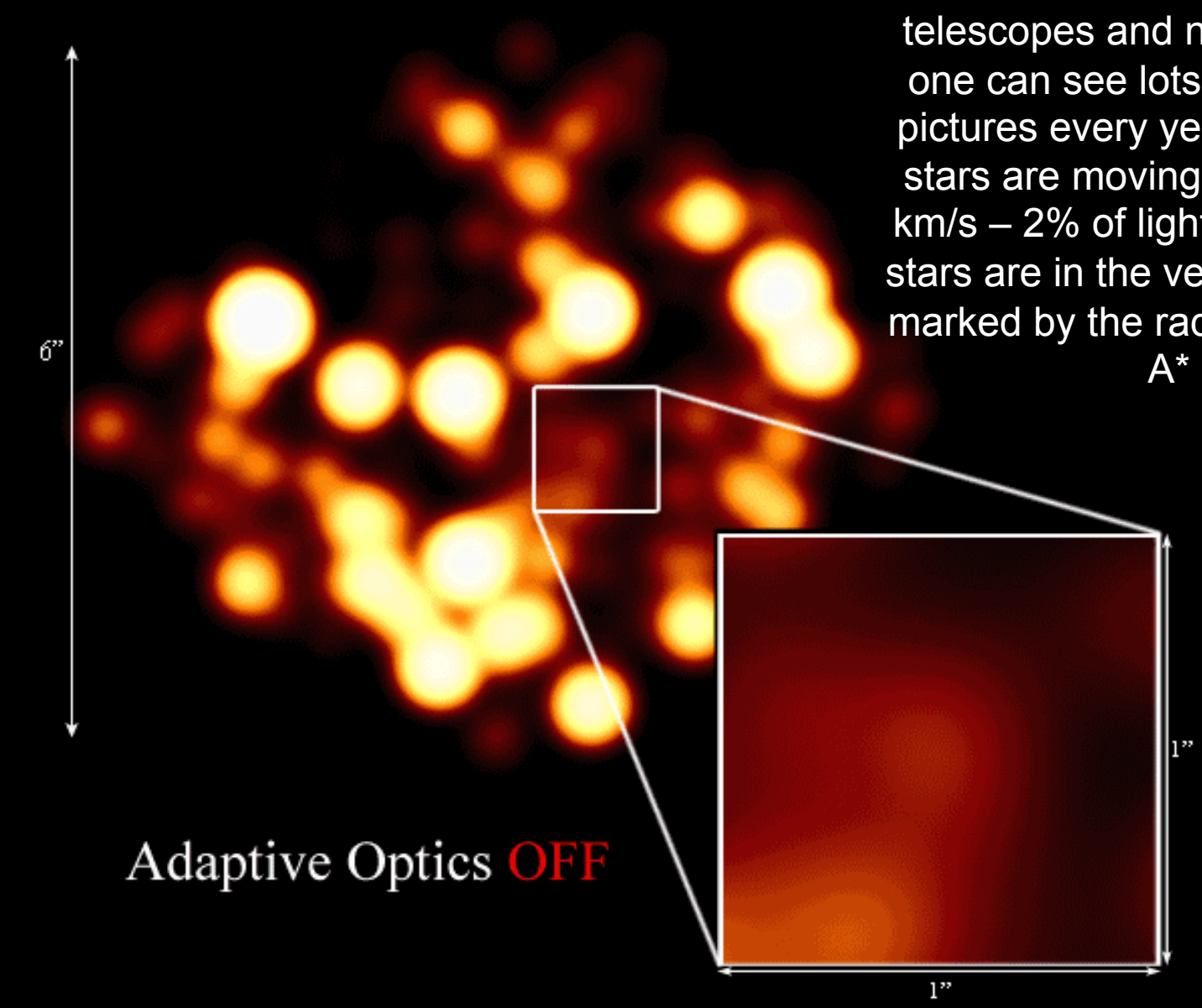

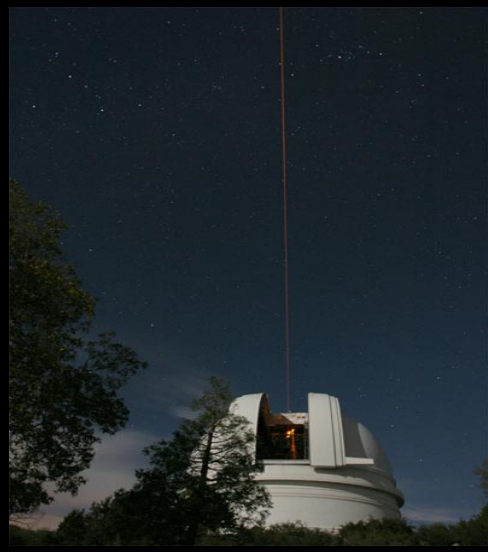

Distance between stars is less that 0.01 pc

Evidence for a *Supermassive* Black Hole at the Galactic Centre

M= 3.6 x 10^6 Solar Masses

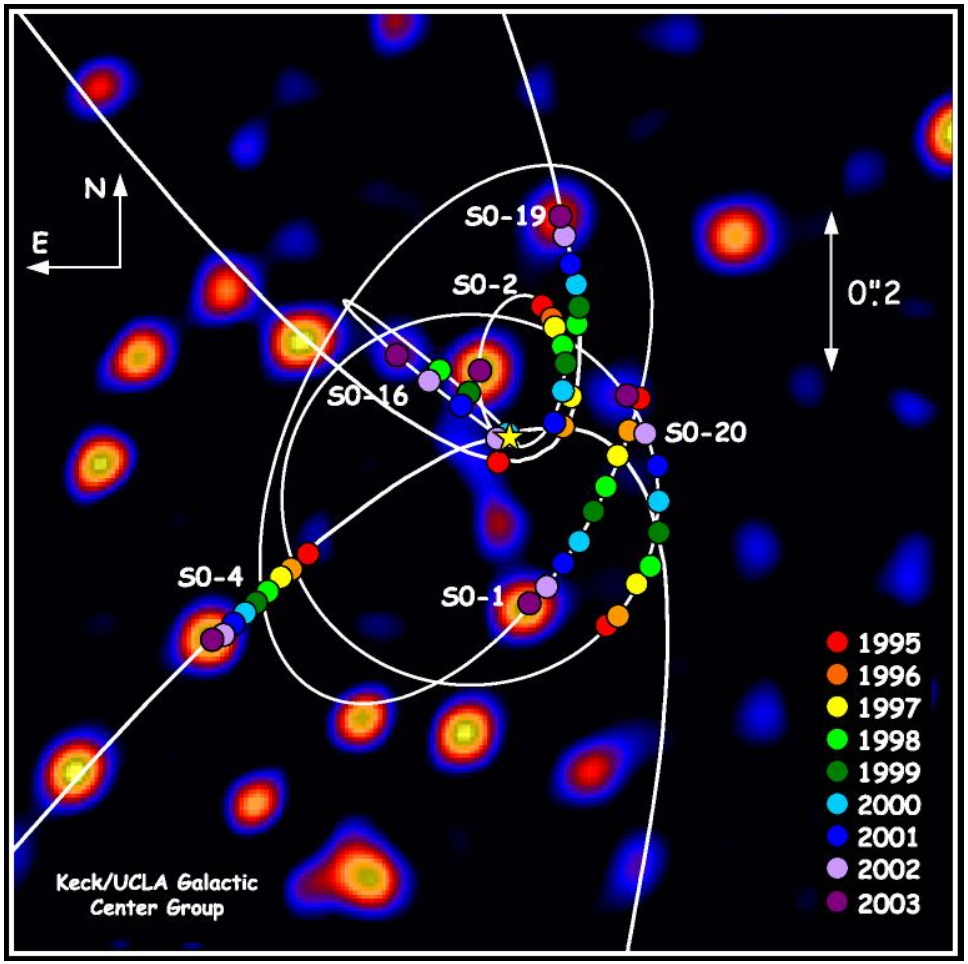

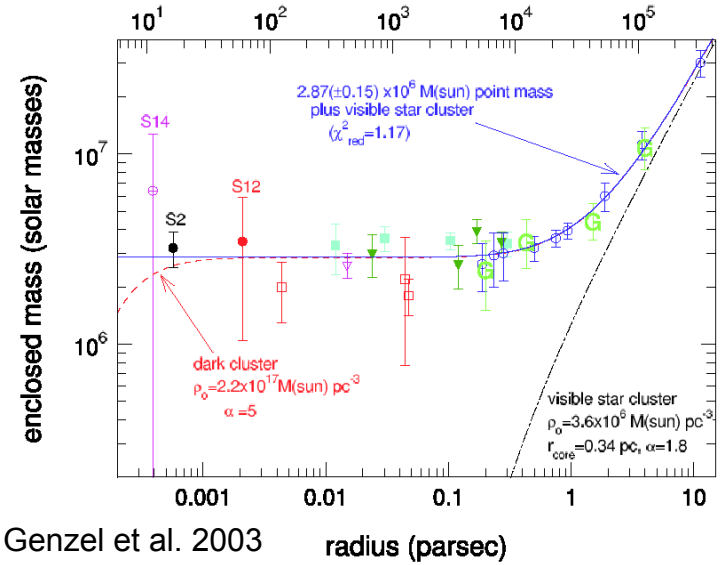

Genzel et al. 2003

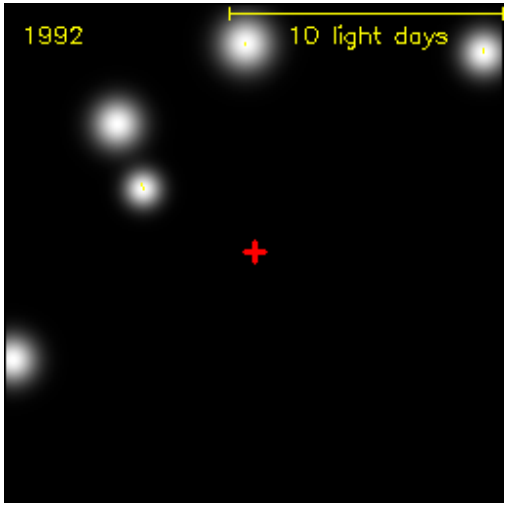

The corresponding Schwarzschild radius is 0.08 AU/12 million km; 17 times bigger than the radius of the Sun

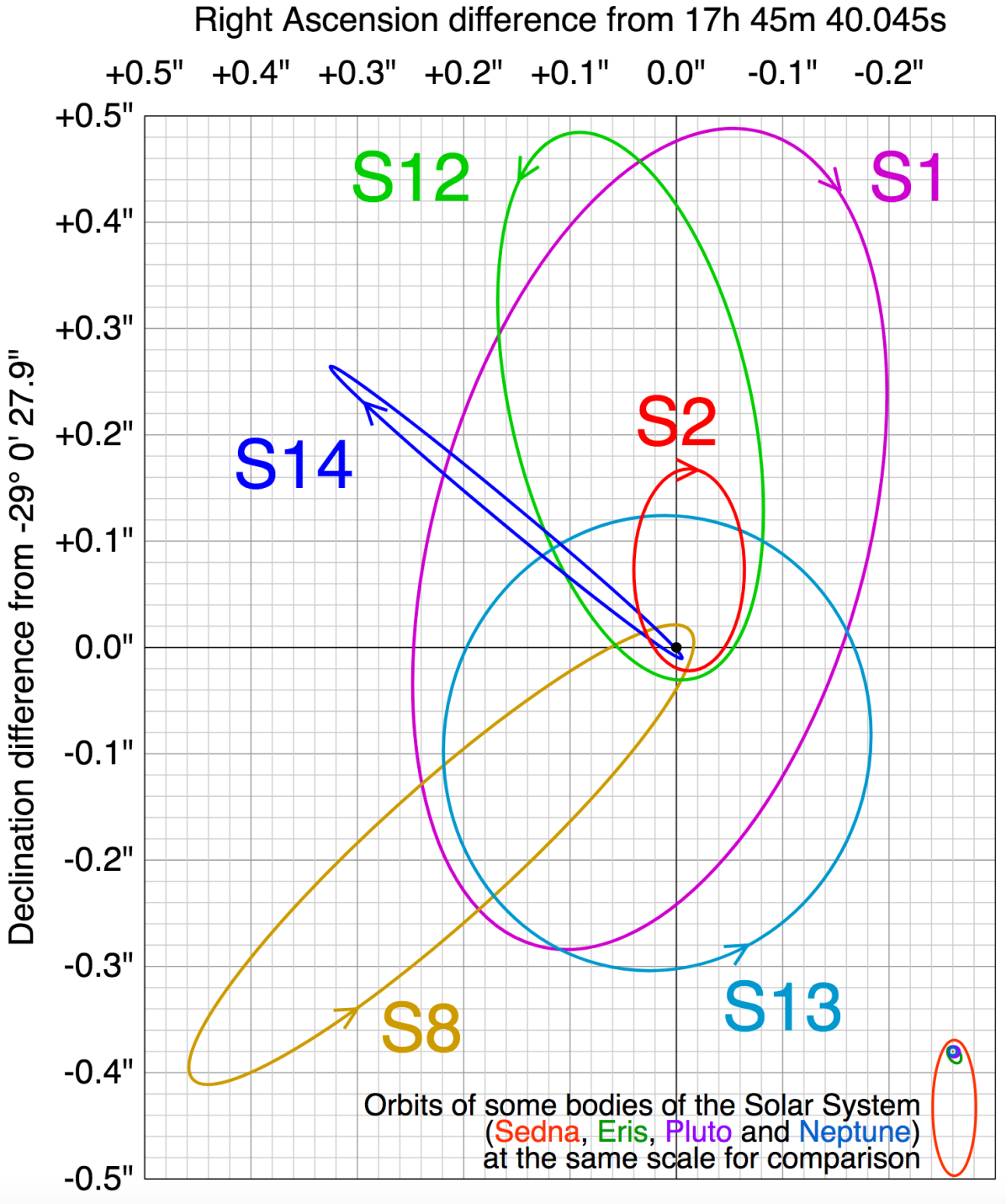
Right Ascension difference from 17h 45m 40.045s
+0.5" +0.4" +0.3" +0.2" +0.1" 0.0" -0.1" -0.2"
Declination difference from -29° 0' 27.9"
+0.5"
+0.4"
+0.3"
+0.2"
+0.1"
0.0"
-0.1"
-0.2"
-0.3"
-0.4"
-0.5"
S12
S1
S2
S14
S13
S8
Orbits of some bodies of the Solar System
(Sedna, Eris, Pluto and Neptune)
at the same scale for comparison

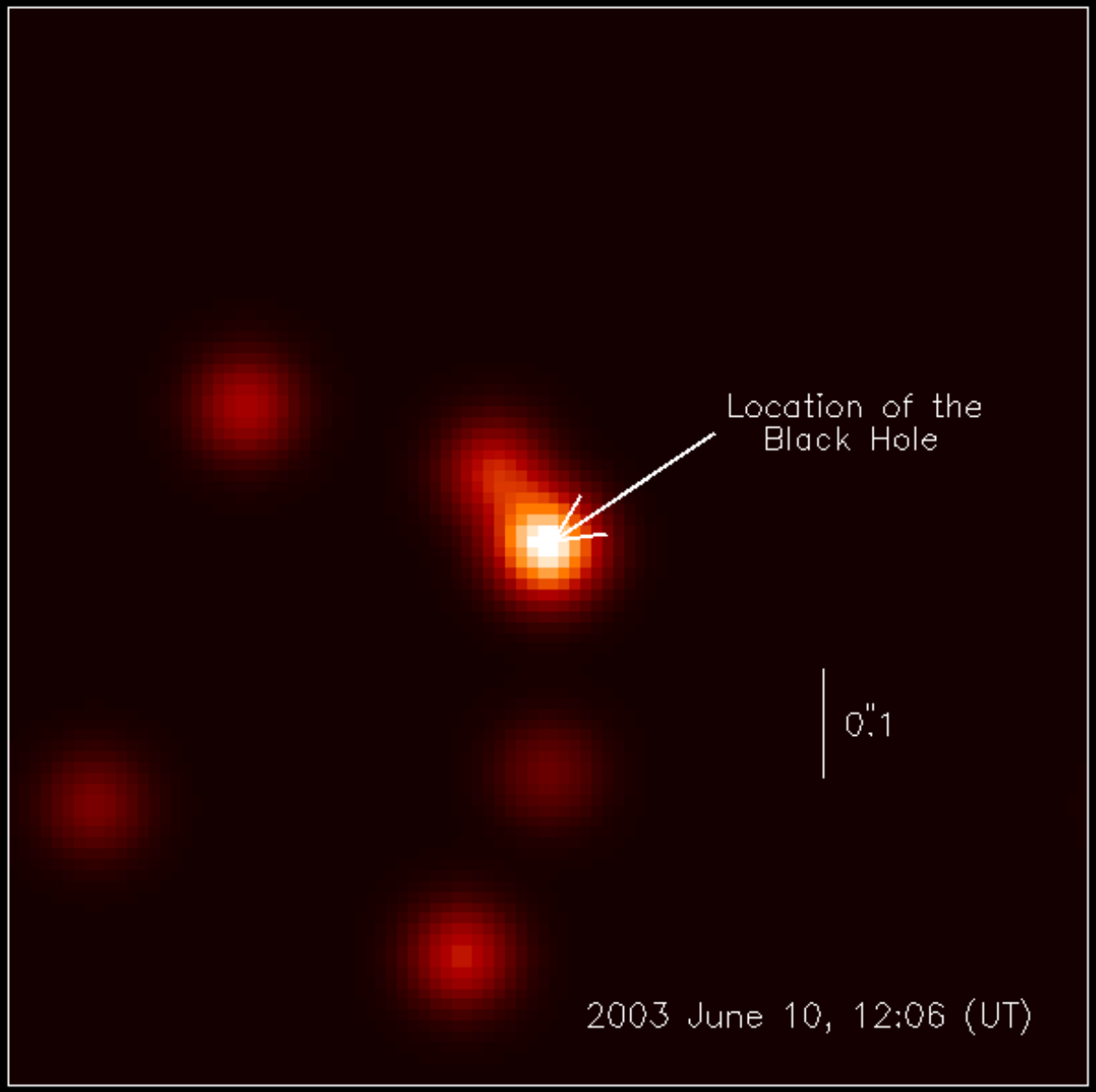
Variable Infrared (3.8 μm) Emission from Sgr A*
Location of the Black Hole
0".1
2003 June 10, 12:06 (UT)

What about X-ray emission due to accretion?

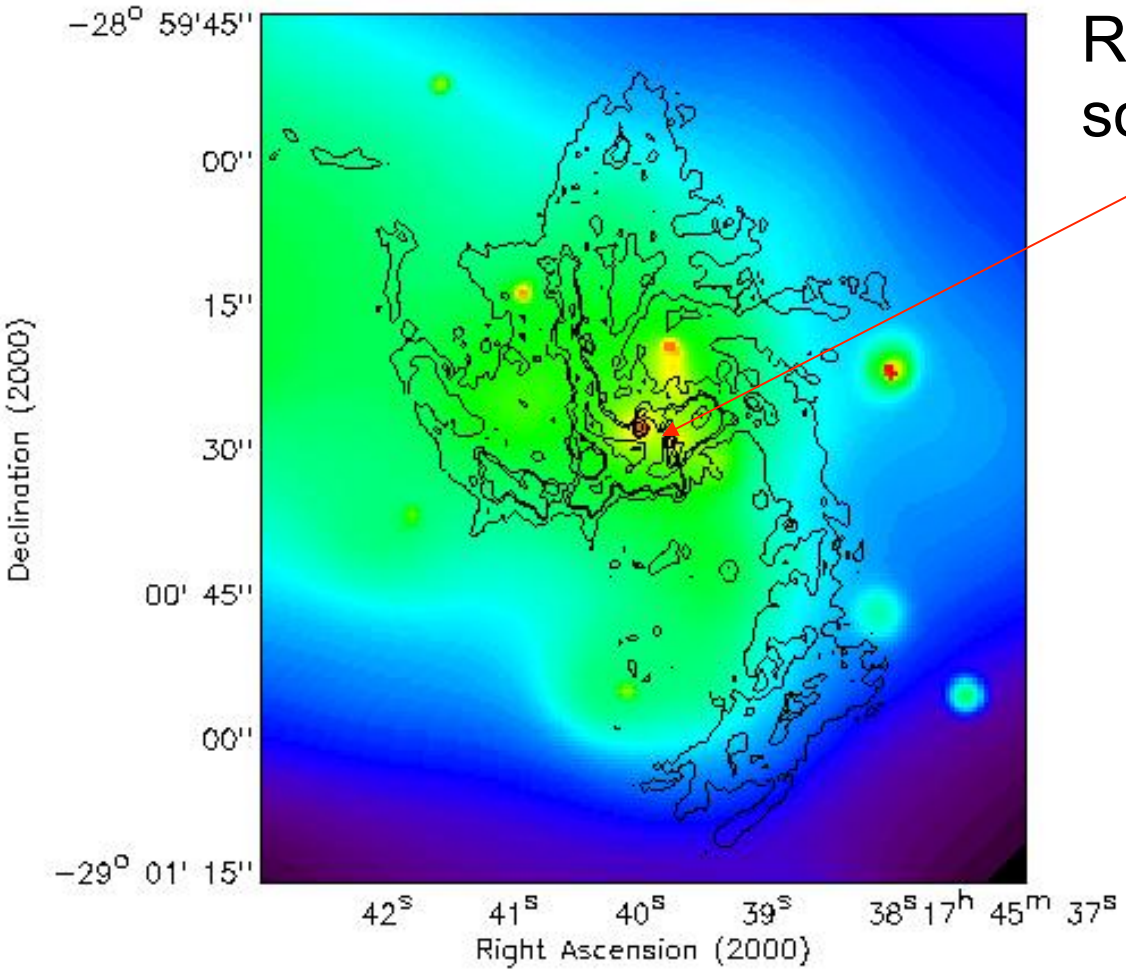

Rather weak X-ray source

Chandra X-ray image of the Sgr A West region

Cores of other galaxies show an accretion disk with a possible black hole

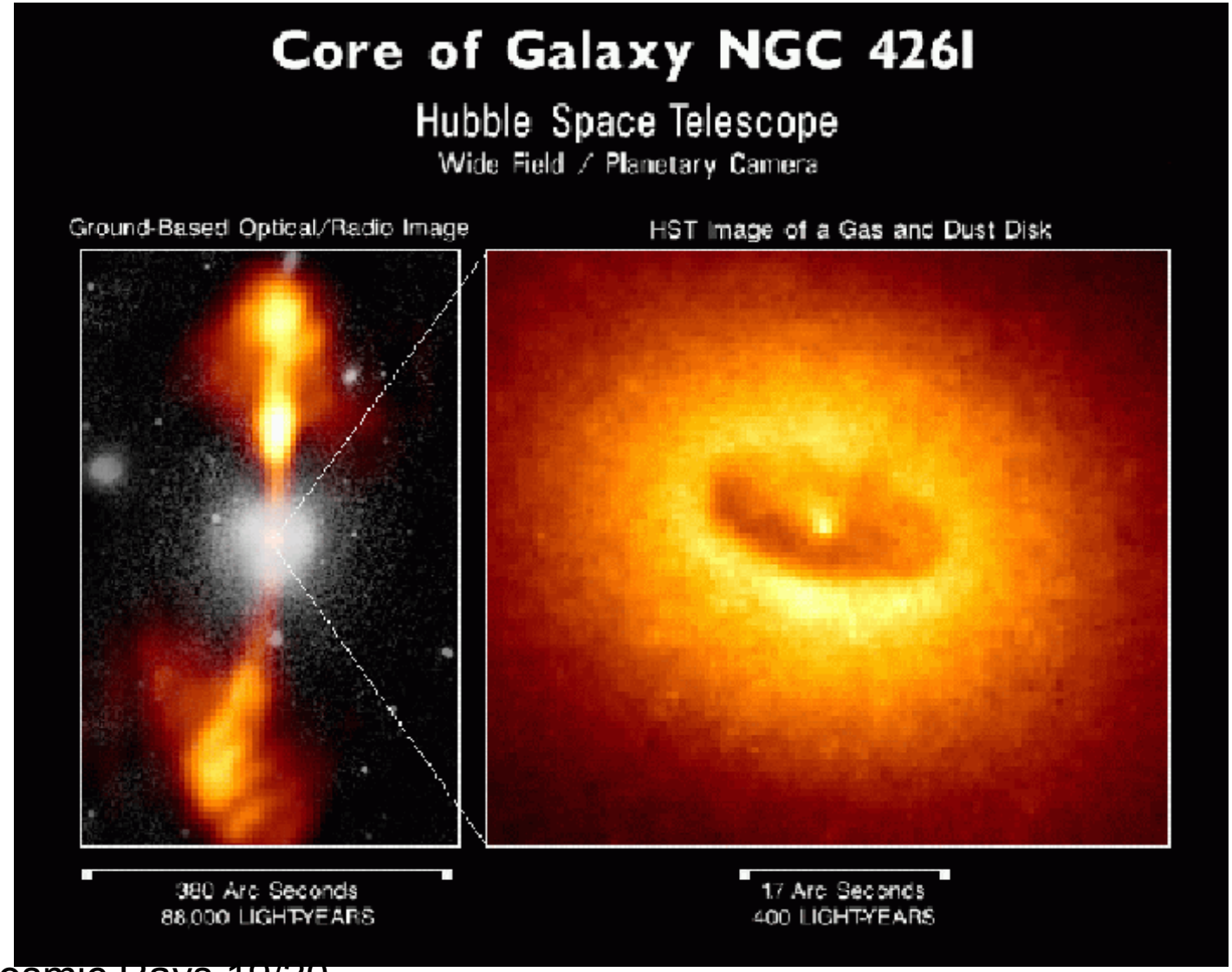

X-ray View of the Galactic Center

Galactic center region contains many black-hole and neutron-star X-ray binaries

Supermassive black hole in the galactic center is unusually faint in X-rays, compared to those in other galaxies

Evidence for a black hole of ~ 3-4 million solar masses:

- Rotation curve indicating an ultra-compact object
- No motion of the central object
- Rapid variability
- Dense stellar population
- Radio jets

Radio jets but rather weak X-ray emission

Other galaxies contain much heavier black holes and stronger activity

What we have learnt:

- Milky way structure: thin spiral disk with a nulear bulge and a large halo
- Cold and Hot gas (mainly H, HI e HII) in the InterStellar Medium (ISM)
- Stars: exploding they supply ISM with matter and energy
- Magnetic fields: large scale structure with many random turbulent irregularities
- Supermassive black hole in the center (?)

Formation and Interactions of CR's

- Now we can have a sketch of CR generation and propagation
- What we are interested in is the CR density for any specie at a given position as a function of time and energy (or momentum), $n_i(\mathbf{x},t,E)$, where i runs over all the elements of the periodic table and $dN_i = n_i(\mathbf{x},t,E)d^3\mathbf{x}dE$

Formation and Interactions of CR's

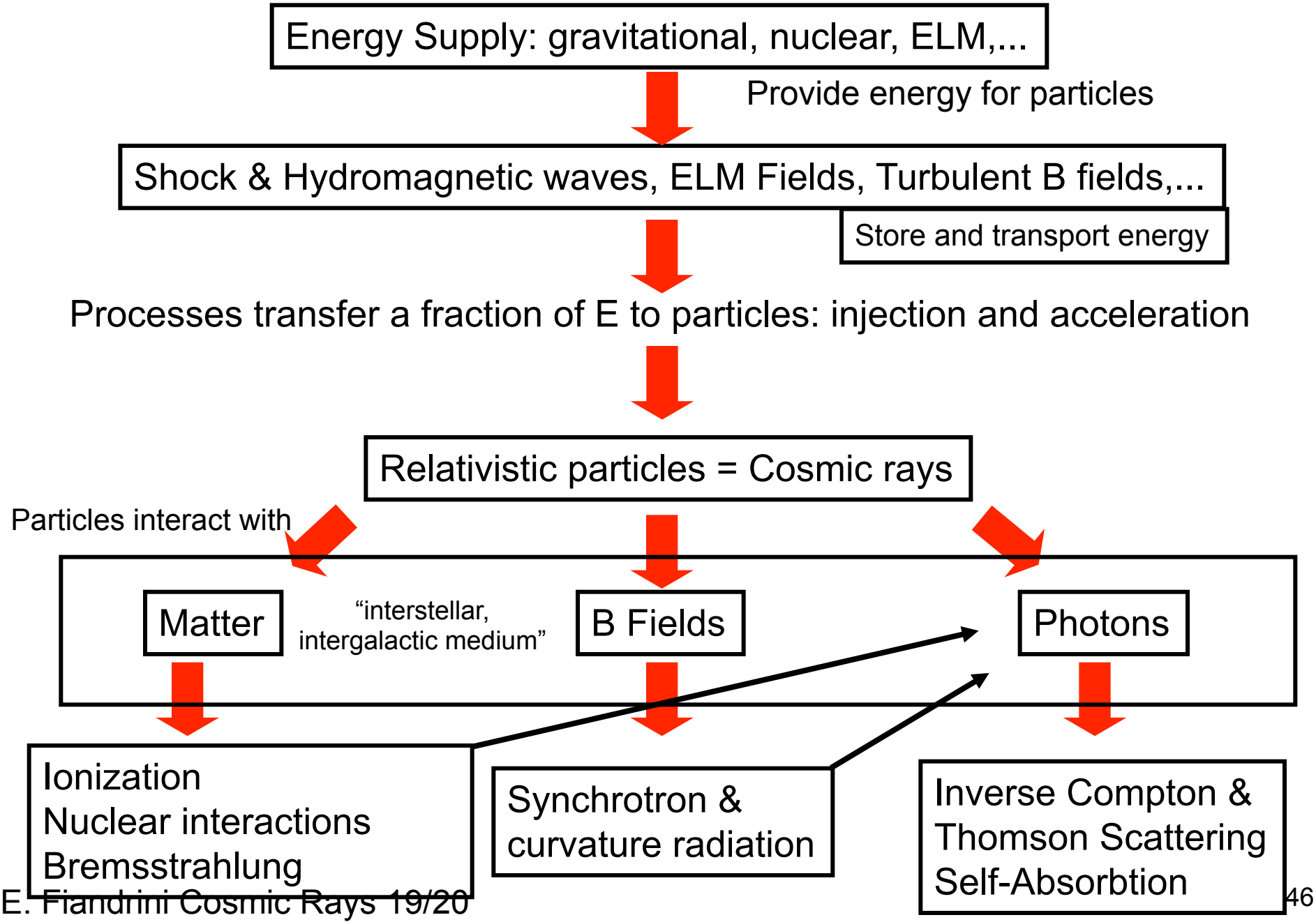

Formation and Interactions of CR's

$$dn_i/dt = \text{Gain} - \text{Loss}$$

Gain = processes that increase the number of particles

Loss = processes that lead to decrease of particles in the phase space volume $d^3\mathbf{x}dE$

$$\frac{\partial n_i}{\partial t} = \left[\text{Gain} - \text{Loss}\right] \text{ in the phase-space cell } d^3x\, dE$$

GAIN

i) Primary sources $q_i(\vec{x}, t, E)$ distribution "Injection spectrum"
(SNR, Pulsars, ...) $\frac{\partial n_i}{\partial t} = q_i$

ii) interactions with ISM: spallation

$$\frac{\partial n_i}{\partial t} = \sum_{j>i} (n_{ISM} \sigma_{ij} \beta c) n_j$$ from heavier particles

iii) Radioactive decay from unstable nuclei

$$\frac{\partial n_i}{\partial t} = \sum_j P_{ij} \frac{n_j}{\tau_j}$$

ϕ) CR are mostly charged → curved by galactic field $\vec{B}$

1) Curvature and gradient drift on $\langle B \rangle$
2) Random motion on $\langle \delta B^2 \rangle$ → Diffusion
3) Convection in the ISM

$$\frac{\partial n_i}{\partial t} = \vec{\nabla} \cdot (\hat{D} \vec{\nabla} n_i + n_i \vec{V}_{ISM})$$

LOSS

i) disintegration by spallation $\frac{\partial n_i}{\partial t} = -n_{ISM} \sigma_{ip} \beta c n_i$

ii) radioactive decay $\frac{\partial n_i}{\partial t} = -\frac{n_i}{\tau_i}$

iii) continous energy loss in the ISM

$$\frac{\partial n_i}{\partial t} = -\frac{\partial}{\partial E}[b(E) n_i]$$

$$b(E) = -\frac{dE}{dt} = \left(\frac{dE}{dt}\right)_{Ion} + \left(\frac{dE}{dt}\right)_{Brems} + \left(\frac{dE}{dt}\right)_{IC+S}$$

(Brems and IC+S terms: → Radiative)

$$\frac{\partial n_i}{\partial t} - \vec{\nabla} \cdot (\hat{D} \vec{\nabla} n_i + n_i \vec{V}_{ISM}) = q_i + \sum_{j>i} \left(n_{ISM} \sigma_{ij} \beta c + \frac{P_{ij}}{\tau_j}\right) n_j - n_{ISM} \sigma_{ip} \beta c n_i - \frac{n_i}{\tau_i} + \frac{\partial}{\partial E}[b(E) n_i]$$

Nature's beam calibration

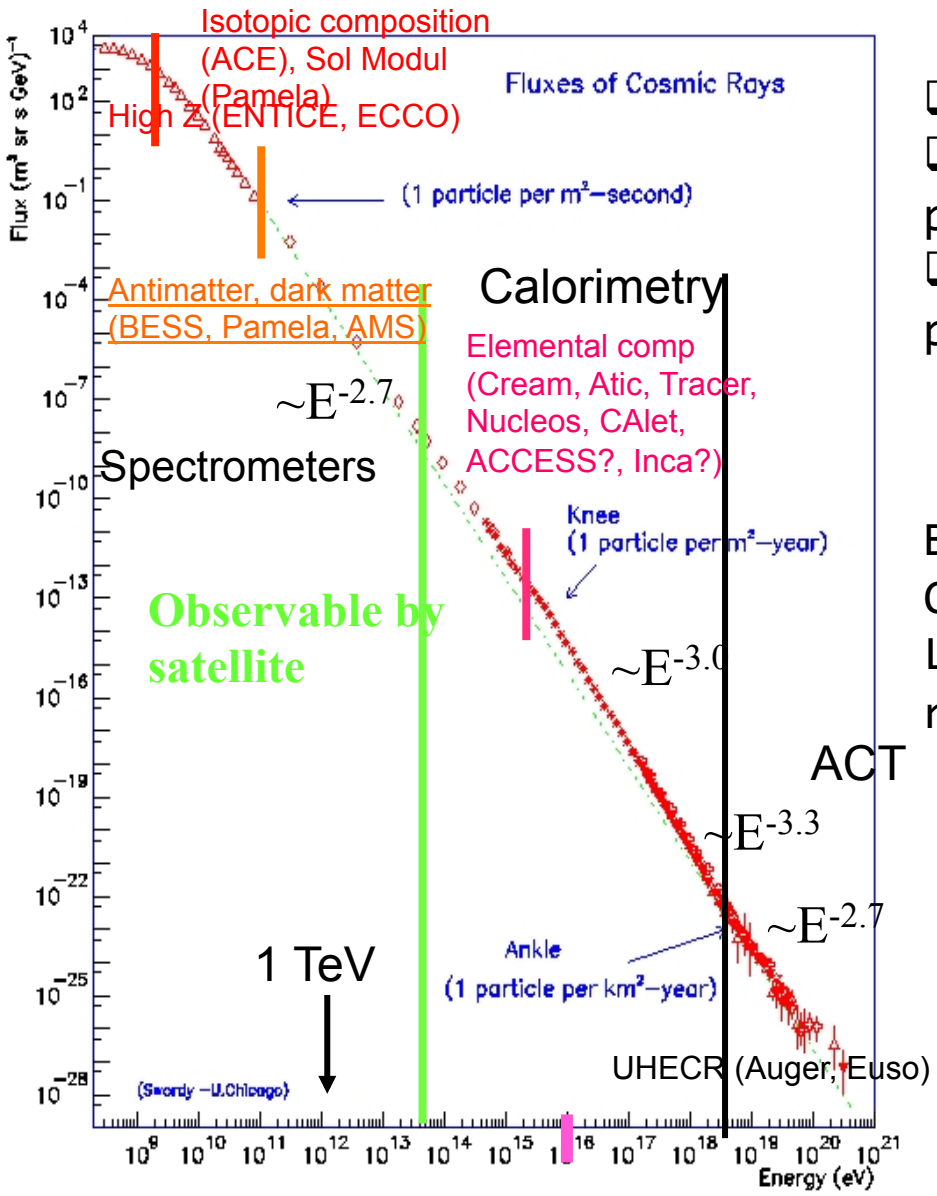

- Nature gives a very energetic beam
- She doesn't give us the beam parameters…
- Get the whole picture → measure precisely the entire CR flux

Beam calibration:

Beam energy←→CR spectrum at Earth

Composition←→CR chemical elements

Luminosity←→CR abundances & reaction rates

Beam Calibration = CR Propagation Models needed for accurate background evaluation of faint signal searches in CR

Beam Calibration = CR Propagation Models

- The goal of the propagation models is to achieve a reliable physical description of the CR production and propagation through the Galaxy
- From the measured fluxes in the heliosphere derive source composition, injection spectra & galactic parameters
- Reliable propagation model is needed for accurate background evaluation for faint signal searches in CR
- Particularly useful measurements to validate propagation models and to constraint their free parameters are flux measurements in a wide energy range of
  - Primary (ratios, eg C/O, fix source abundances)
  - Secondary (secondary to primary ratios, eg B/C, fix the grammage crossed, constraint diff coeff and halo thickness)
  - Radioactive (provide, eg $^{10}Be/^{9}Be$, escape time information)

Abbondanze degli elementi nella Galassia

- Le abbondanze “primordiali” degli elementi sono fissate dalla **nucleosintesi primordiale**:
  - 24% (in massa) di 4He
  - 76% (in massa) di H
- La **nucleosintesi** nelle stelle provvede alla sintesi degli elementi più pesanti
- Le esplosioni stellari (per M>> Ms) hanno una vita media << all’età dell’Universo e provvedono a rifornire il mezzo interstellare
- Le percentuali dei vari elementi nella Galassia possono essere dedotte in varie maniere

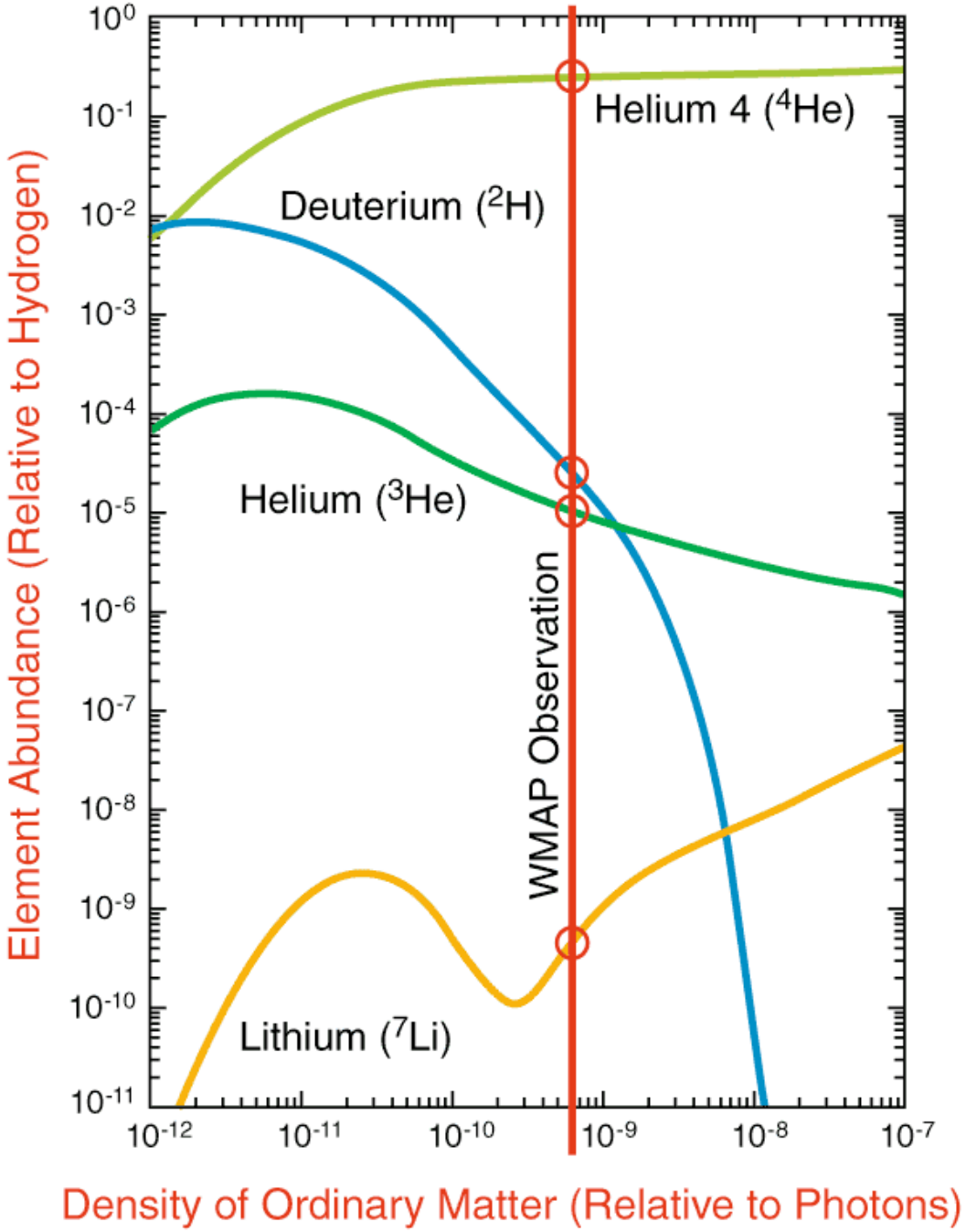

NASA/WMAP Science Team
WMAP101087

Element Abundance graphs: Steigman, Encyclopedia of Astronomy and Astrophysics (Institute of Physics) December, 2000

Chemical composition

Cosmic rays contain all the elements of the periodic table

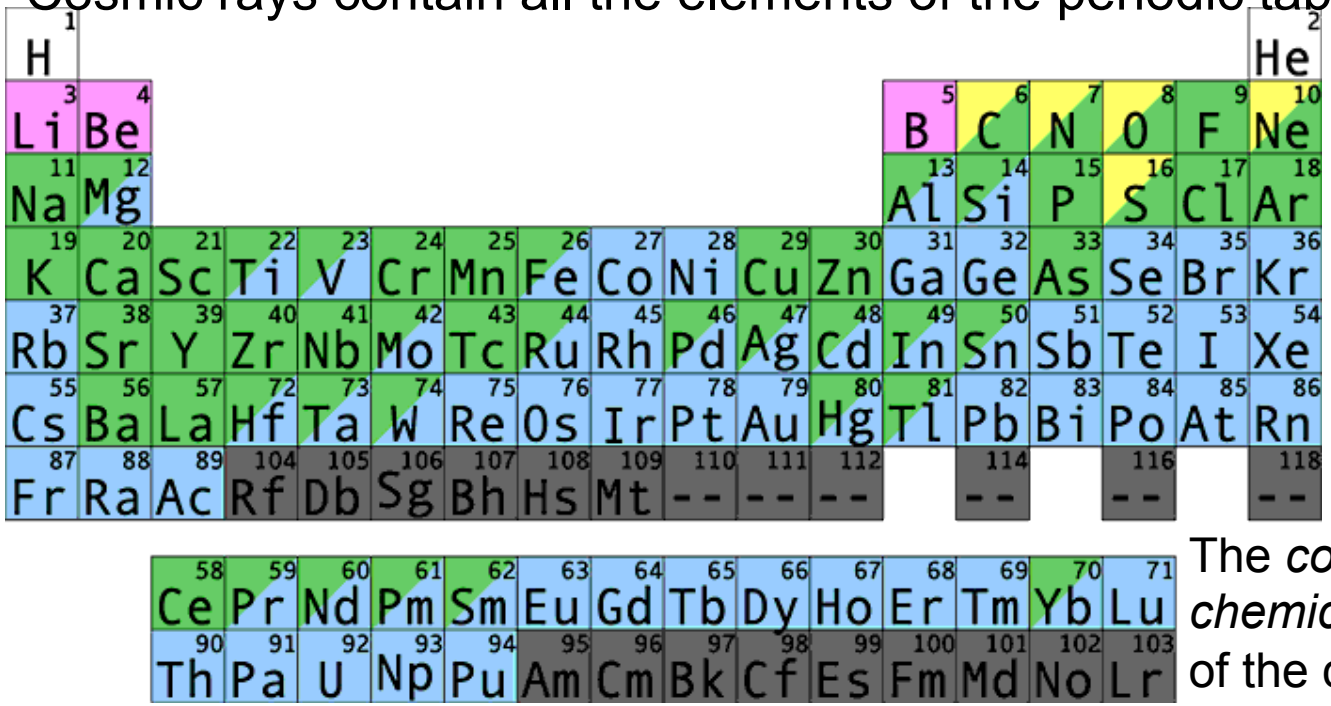

White - Big Bang
Pink - Cosmic Rays
Yellow - Small Stars
Green - Large Stars
Blue - Supernovae

The *cosmochemistry* or *chemical cosmology* is the study of the chemical composition of matter in the Universe and the processes that led to the observed compositions. Meteorites and photospheric measurements of solar light are one of the most important tools for studying the chemical nature of the Solar System.

Abundances in Solar System

They are representative of the abundances in the ISM

the chemical composition of the solar system is representative of the part of the Galaxy (the disk) with equal evolution history and the term *cosmic abundances* is sometimes used as a synonym for solar system abundances

o/ph:

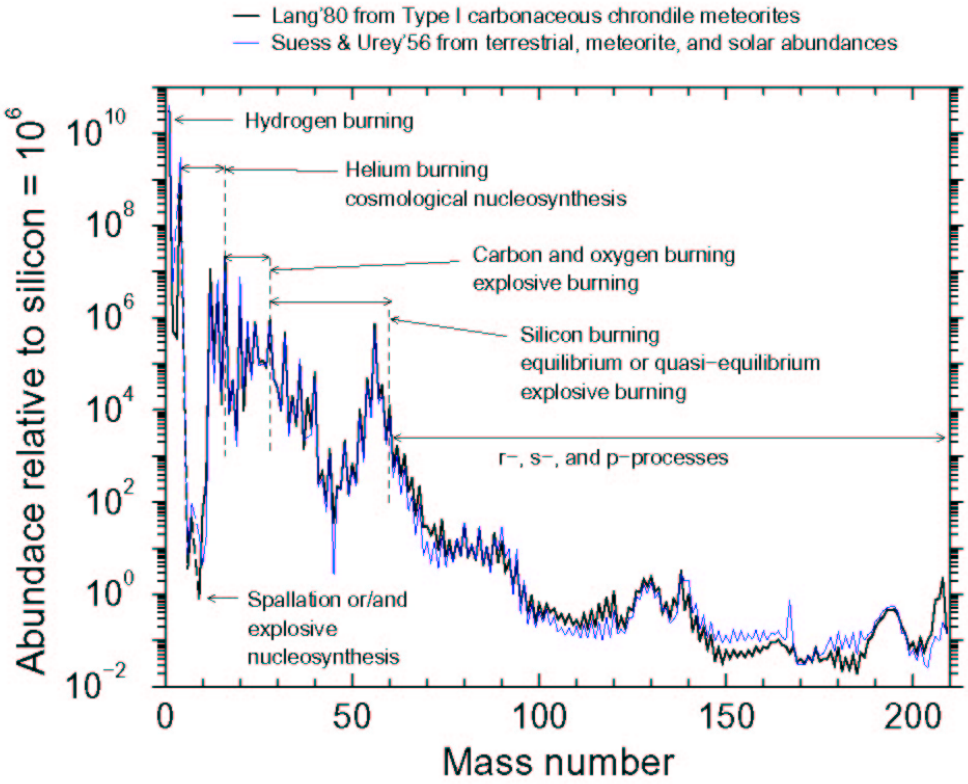

Fig. 1.— Abundances of solar system nuclides plotted as a function of mass number. The thin blue curves shows old data compiled in Table III by Suess and Urey (1956) which are based on measurements of terrestrial, meteoric, and solar abundances. These data were used by Burbidge, Burbidge, Fowler, and Hoyle (1957) in postulating the basic nucleosynthetic processes in stars in their seminal work which become widely known as "B^2FH," the "bible" of nuclear astrophysics. The thick black curve shows newer data from the compilation published in Table 38 by Lang (1980) which are based upon measurement of Type I carbonaceous chrondite meteorites, and are thought to be a better representation than Suess and Urey's curve. The nuclear processes which are thought to be the main stelar mechanisms of nuclide production are shown as well in the figure.

Confronto tra le abbondanze dei vari nuclidi nei RC e nell'ISM

- I RC hanno una composizione chimica analoga a quella del Sistema Solare (Solar System Abundance, SSA)?
- Se sì, questo indica una origine simile a quella del SS.
- Le abbondanze degli elementi nei RC si determinano tramite esperimenti di misura diretta dei RC (vedi.)
- Si notano alcune discrepanze rispetto al SSA, in particolare in corrispondenza al gruppo Li, Be, B e del gruppo prima del Fe → Vedi fig.
- Si nota anche un effetto *pari/dispari*, noto dalla fisica dei nuclei

Abbondanze relative dei RC e del sistema solare (SSA)

- H e He sono dominanti (98%), leggermente in difetto rispetto SSA
- Buon accordo tra CR e SSA per molti elementi, in particolare C, O, Mg, Fe.
- Elementi leggeri Li, Be, B e quelli prima del ferro Sc,V sono straordinariamente abbondanti nei RC rispetto SSA

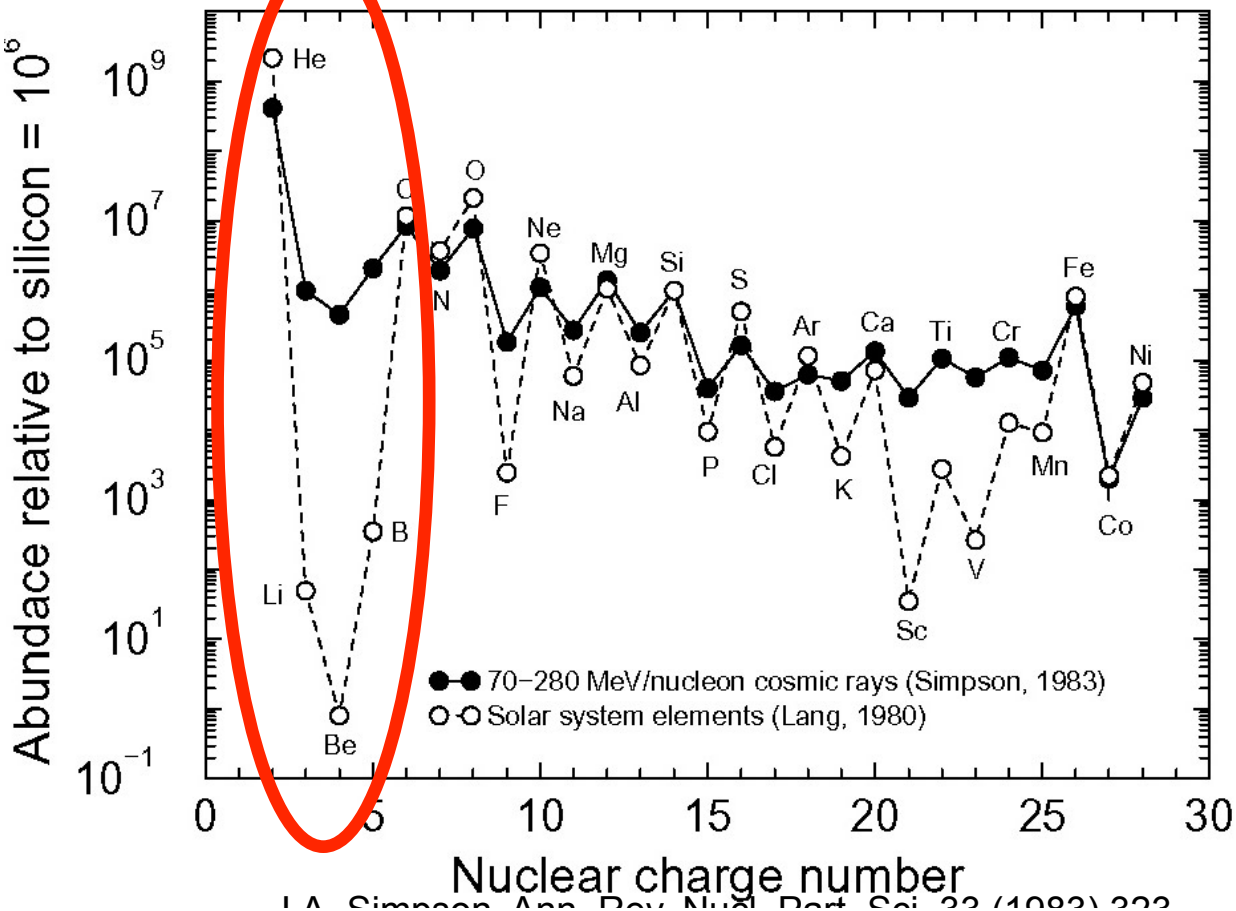

The first conclusion from the data shown is that the accelerated matter arriving on Earth is sampled from a region whose surrounding material has the same chemical composition of our Solar System. This material is plausibly originated by the same mechanism that originated the Sun and the planets, with some exceptions

La composizione Chimica : confronto tra il elementi prima e dopo il Fe

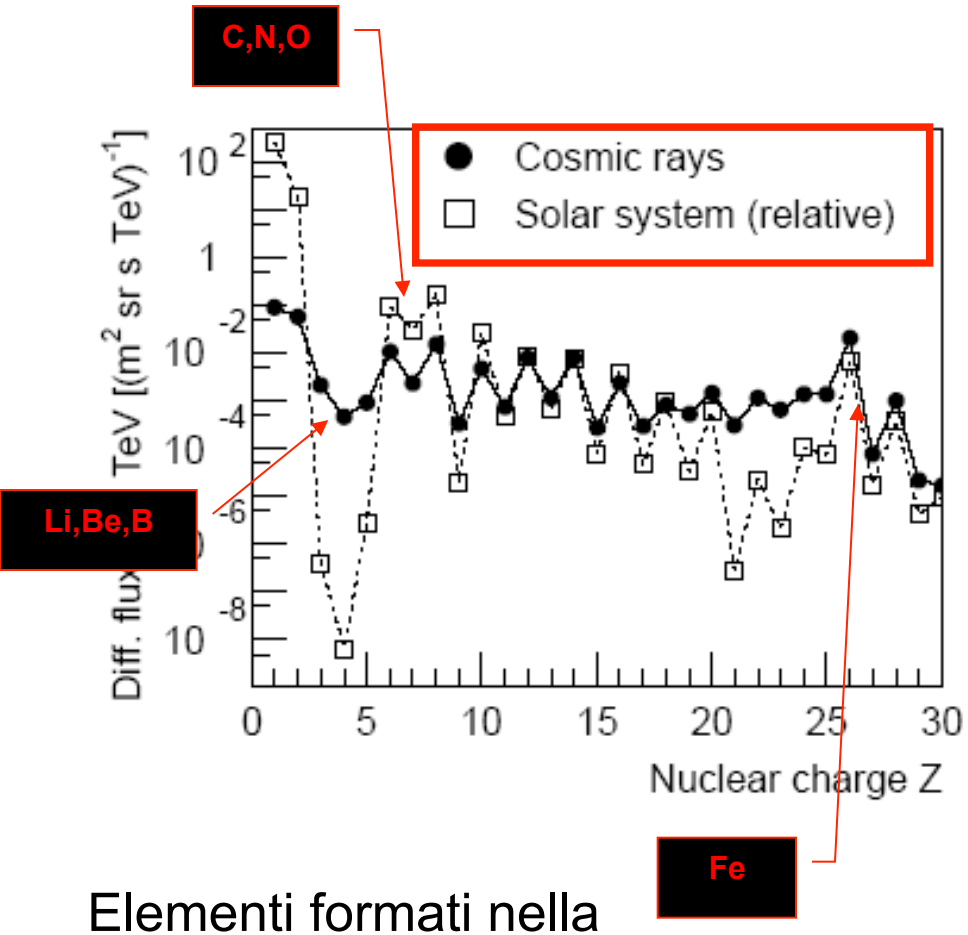

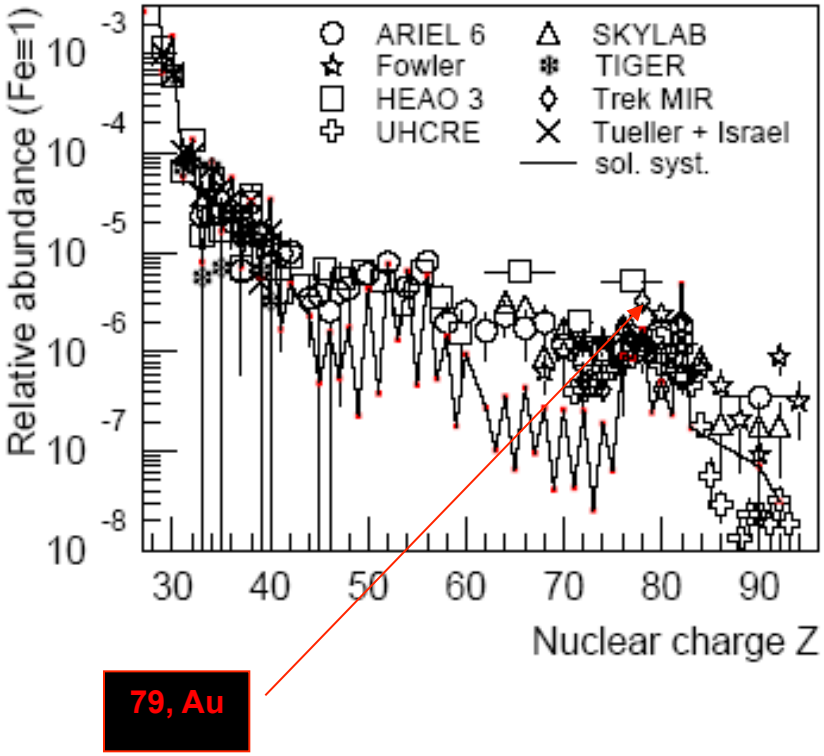

Elementi formati nella Nucleosintesi stellare

Elementi formati nell'esplosione (supernova)

La stessa figura…

In addition to stable isotopes, CRs contain long-lived radioactive nuclides, mostly of secondary origin. The observed abundances of these isotopes can be used for establishing various time scales related to the origin of CRs. In particular, secondary isotopes which decay through β± emission have been used as a second method to measure the residence times of CR in the galaxy, τ_{esc}.

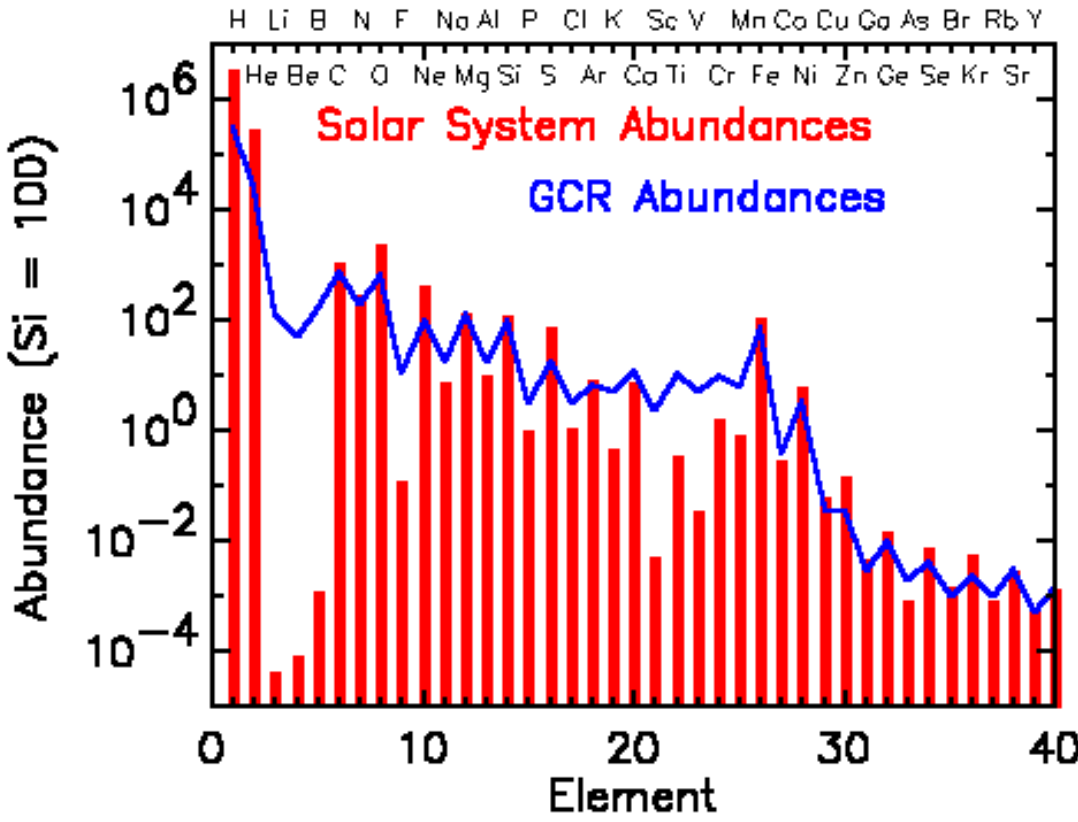

CHEMICAL COMPOSITION of CR at LOW ENERGIES

Intensity (E > 2.5 GeV/particle(m^{-2} sr^{-1} sec^{-1})

Nuclear group	Particle charge, Z	Integral Intensity in CR (m^{-2} s^{-1} sr^{-1})	Number of particles per 10^4 protons	
			CR	Universe
Protons	1	1300	10^4	10^4
Helium	2	94	720	1.6×10^3
L (=Li,Be,B)	3-5	2	15	10^{-4}
M(=C,N,O)	6-9	6.7	52	14
Heavy	10-19	2	15	6
VeryHeavy	20-30	0.5	4	0.06
SuperHeavy	>30	10^{-4}	10^{-3}	7×10^{-5}
Electrons	-1	13	100	10^4
Antiprotons	-1	>0.1	5	?